

Distribution Agreement

In presenting this thesis as a partial fulfillment of the requirements for a degree from Emory University, I hereby grant to Emory University and its agents the non-exclusive license to archive, make accessible, and display my thesis in whole or in part in all forms of media, now or hereafter known, including display on the World Wide Web. I understand that I may select some access restrictions as part of the online submission of this thesis. I retain all ownership rights to the copyright of the thesis. I also retain the right to use in future works (such as articles or books) all or part of this thesis.

Signature:

Mark Harousseau

April 10th, 2012

The Role of Polymerase δ Interacting Protein 2 in Neointima Formation

by

Mark Harousseau

Dr. Kathy Griendling
Adviser

Emory University School of Medicine
Department of Cardiology

Dr. Kathy Griendling
Adviser

Dr. Arri Eisen
Committee Member

Dr. Bill Kelly
Committee Member

Date

The Role of Polymerase δ Interacting Protein 2 in Neointima Formation

By

Mark Harousseau

Dr. Kathy Griendling

Adviser

An abstract of
a thesis submitted to the Faculty of Emory College of Arts and Sciences
of Emory University in partial fulfillment
of the requirements of the degree of
Bachelor of Sciences with Honors

Department of Biology

2012

Abstract

The Role of Polymerase δ Interacting Protein 2 in Neointima Formation

By Mark Harousseau

The process of restenosis, or renarrowing of an injured artery, results in the proliferation and migration of vascular smooth muscle cells (VSMCs) into the intima, forming the neointima. The pathological mechanism of neointima formation is complex and is believed to involve multiple cellular mechanisms including migration, proliferation, apoptosis, and extracellular matrix (ECM) formation. Polymerase δ interacting protein 2 (Poldip2, also known as PDIP38 and Mitogenin I) is a multifunctional protein that regulates DNA repair, cytoskeletal remodeling, proliferation, and the generation of reactive oxygen species, products of oxygen metabolism in all aerobic systems, via its interaction with the NADPH oxidase Nox4. This latter function may be particularly relevant to vascular pathology, as Nox4 regulates phenotypic differentiation and migratory function of VSMCs. Little is known about the functionality of Poldip2. Here, using a Poldip2 (+/-) gene trap animal model and a transluminal wire injury model with rapid onset of medial cell apoptosis and replicable neointimal hyperplasia ~3-4 weeks post injury, we demonstrate that Poldip2 heterozygosity results in reduced neointima area, an increased deposition of an ECM component within the neointima and a trend of decreased proliferation in injured femoral arteries of Poldip2 (+/-) mice compared to wildtype (WT) mice. We also demonstrate that Poldip2 expression does not affect apoptosis, which mediates the initial vessel response to injury. Our findings implicate Poldip2 as an important regulator of neointima formation, and demonstrate that it exerts its effects via multiple cellular mechanisms. Future

studies should be designed to delve further into these mechanisms in order to design therapeutic agents to treat the clinically important problem of restenosis.

The Role of Polymerase δ Interacting Protein 2 in Neointima Formation

By

Mark Harousseau

Dr. Kathy Griendling

Adviser

A thesis submitted to the Faculty of Emory College of Arts and Sciences
of Emory University in partial fulfillment
of the requirements of the degree of
Bachelor of Sciences with Honors

Department of Biology

2012

Acknowledgements

Firstly, I would like to thank my adviser, Dr. Kathy Griendling, for her guidance and generosity in allowing me to complete this project. I would like to thank Dr. Srinivasa Raju Datla for his constant guidance and knowledgeable support during my research. Additionally, I would like to thank other members of the Griendling Laboratory that were integral to this process, including Dr. Candace Adamo, Dr. Bernard Lassègue, Dr. Abel Garrido, Dr. Mazen Khalil, Dr. Bonnie Seidel-Rogol, and Holly C. Williams. I am also very thankful for the help of Dr. Lu Hilenski, the Director of the Internal Medicine Imaging Core, and Giji Joesph, from the Taylor Laboratory, for their time and advice. I would also like to thank my committee members, Dr. Arri Eisen and Dr. Bill Kelly, for their suggestions and assistance. Lastly, I would like to thank my family and friends for their support during this whole entire process.

Table of Contents

Introduction	1-10
Materials and methods	11-18
a. Animals	11
b. Transluminal wire Injury	12
c. Tissue collection and slide preparation	13
d. Collagen Staining	13
e. Apoptosis	14
f. Proliferation detected by immunofluorescent histology	14
g. Smooth muscle α -actin immunolabeling	15
h. <i>In vitro</i> studies	15
i. Microscopy	16
j. Image analysis and calculations	16
k. Statistical analysis	17
Results	19-35
a. Poldip2 (+/-) heterozygosity and neointimal reduction	19-21
b. <i>In vitro</i> ECM protein studies	21-22
c. <i>In vivo</i> characterization of collagen	22-24
d. Medial Layer Apoptosis	25-26
e. siPoldip2 limits proliferation <i>in vitro</i>	27
f. Optimizing PCNA Immunolabeling	27-30
g. Proliferation within the medial layer and neointima following wire injury	30-35
h. Cellular counts within the medial layer and neointima	35-36
i. Vascular smooth muscle cell localization	36-37
Discussion	38-46
References	47-50

List of Figures

Figure 1- The formation of neointimal hyperplasia	3
Figure 2- Interruption of the Poldip2 gene at intron 1	11
Figure 3- Timeline of femoral artery collection	12
Figure 4- The ratio of intima to media layer areas	20
Figure 5- Haematoxylin and Eosin staining of wiltype and Poldip2 (+/-) uninjured and wire-injured femoral arteries	21
Figure 6- <i>In vitro</i> ECM protein production	22
Figure 7- Picrosirius Red Stain for Collagen	23
Figure 8- Collagen deposition measurement in the neointima using ImageJ Software	24
Figure 9- Collagen Deposition in the Neointima	24
Figure 10- Medial layer apoptosis two hours post wire-injury	26
Figure 11- Poldip2 has no effect on medial layer cell death	26
Figure 12- siPoldip2 treatment inhibits smooth muscle cell proliferation	27
Figure 13- Optimization of PCNA immunolabeling	30
Figure 14- Proliferation one week post wire injury as assessed by immunofluorescent labeling for PCNA	32
Figure 15- Proliferation two weeks post wire injury as assessed by immunofluorescent labeling for PCNA	33
Figure 16- Proliferation three weeks post wire injury as assessed by immunofluorescent labeling for PCNA	34
Figure 17- Percent proliferation within the neointima and medial layers of both animal groups	35
Figure 18- Cellular counts within the AOIs of each animal group	36
Figure 19- Smooth muscle cell α -actin immunolabeling	37

INTRODUCTION

According to the CDC's preliminary 2010 National Vital Statistics Report, diseases of the heart are the leading cause of death and are responsible for approximately 24.1% of all deaths in the United States.¹ Even though substantial clinical advancements have been made in preventative cardiac care, the incidence rates of these diseases are of epidemiologic urgency. In fact, inpatient cardiovascular operations and procedures have increased by 27% between 1997 and 2007.² Yet, nearly 33% of deaths due to cardiovascular disease (CVD) occur before the age of 75, which is below the average life expectancy of 77.9 years.^{2,3} The scope of cardiovascular disease covers the incidence of atherosclerosis, stroke, myocardial infarctions (MI), coronary heart disease and post-angioplasty restenosis, the condition of interest in this paper.

In 2004, 1.2 million hospital stays were attributed to coronary atherosclerosis, for which over half of the patients received some form of percutaneous coronary intervention.² The arterial condition atherosclerosis is of substantial importance due to its principal role in MIs, angina pectoris, cerebral infarctions, arterial thrombosis, and other conditions based on the circulatory region affected.^{4,5} Its clinical manifestation is often only observable when the condition has developed to a chronic or acute clinical expression. The temporal progression of atherosclerosis from the initial lesion to clinically observable manifestations can take years. The importance of understanding the mechanism of its initiation and progression is of great value for clinical and scientific advancement, and even though significant progress has been made in the last decade, many details still remain unexplained.

The difficulty of early atherosclerotic treatment is entirely due to the nature of the disease. As mentioned, the prolonged development of the disease makes early detection difficult, especially when many cases never reach clinical significance. The stenotic phenotype, when

chronic, can often occur focally at predisposed locations, but the nonocclusive instances of atherosclerosis can occur diffusely throughout the affected arteries.⁴ These quiescent phases of atherosclerosis often go unnoticed until postmortem discovery. Clinically chronic manifestations, however, are often treated with corrective measures such as angioplasty or graft placement for urgent response.

Angioplasties revolutionized the field of preventive cardiac medicine in the treatment of prolonged stenosis in cardiovascular disease. In 2007 alone, 622,000 patients underwent percutaneous coronary intervention (PCI).² Post-angioplasty restenosis, however, is a common complication of this minimally invasive procedure, and limits the post clinical success of the procedure.⁶ Understanding the physiological manifestations of atherosclerosis, a causative agent of PCI, and restenosis, a negative outcome of PCI, is integral to being able to clinically limit the pathological impact of these conditions, especially when atherothrombotic diseases are projected to be the leading cause of death worldwide by 2020.²

The biology of the vessel wall is an indispensable part of this story. Normal muscular and elastic arteries are made up of three distinct layers: the intima, the media, and the adventitia. The intimal layer is the innermost layer and consists of a single layer of endothelial cells on the luminal side, a narrow layer of extracellular connective matrices, and the internal elastic lamina, a sheath of elastic fibers, on the peripheral side.⁴ The medial layer consists of vascular smooth muscle cells (VSMCs), differing amounts of collagen, and proteoglycans.⁴ Lastly, separated from the medial layer by the external elastic lamina, the adventitia is the outermost layer and is composed of fibroblasts and smooth muscle cells intermixed in a matrix of collagen and proteoglycans.⁴ The independent roles of each these layers in cardiovascular pathology are interconnected, and will each be addressed to an extent.

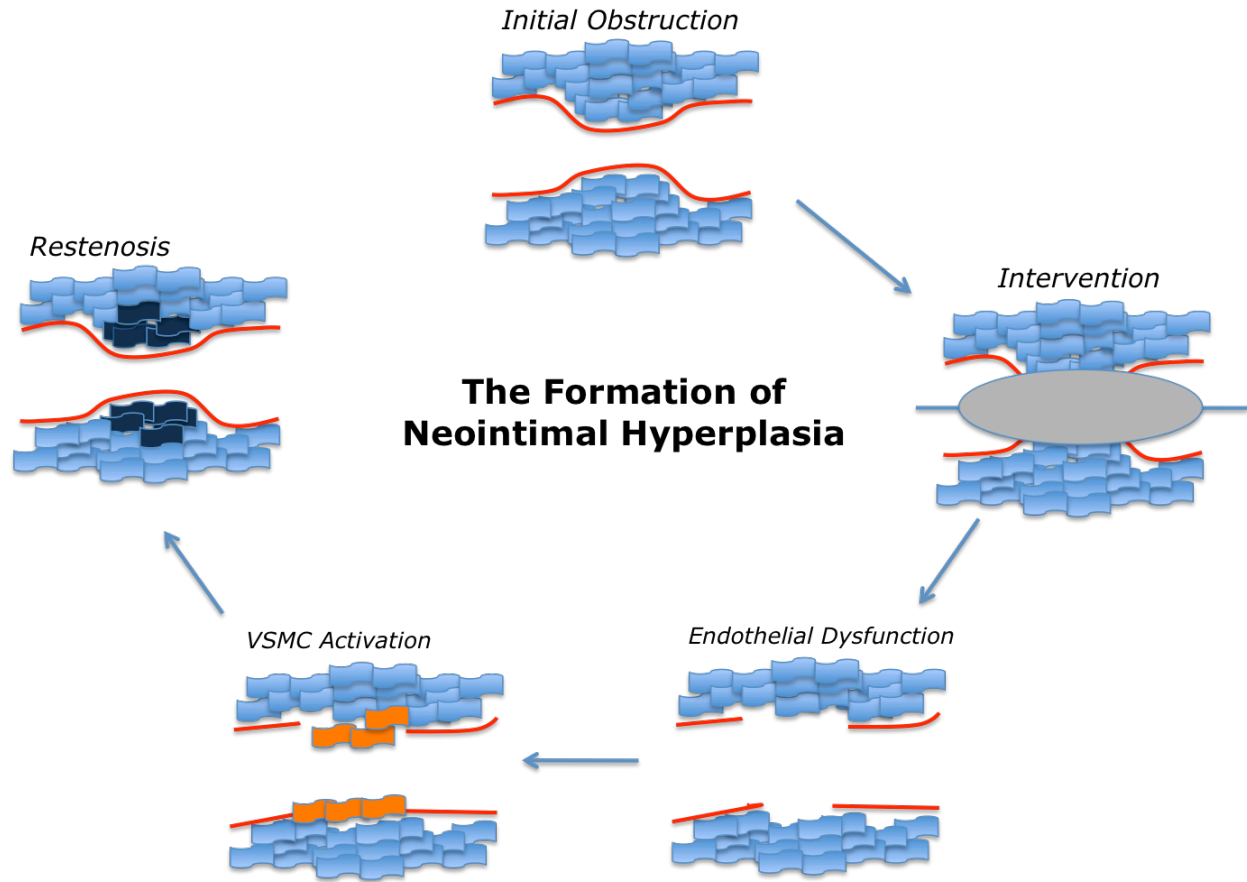


Figure 1- The onset of neointimal hyperplasia and the development of restenosis following vascular injury. Adapted from Popowich et al.⁷

Restenosis

The process of restenosis, or renarrowing of an artery after treatment, culminates in neointima formation characterized by the proliferation and migration of VSMCs into the intima and ECM formation (Figure 1).⁸ It is triggered by arterial wall injury induced by removal of the endothelial layer and physical stretching of the arterial wall. The loss of endothelial function is a frequent occurrence in many cardiovascular diseases. Normal endothelial function is integral in maintaining vasodilatation and inhibiting contraction, thrombosis, white blood cell adhesion, and vascular smooth muscle growth.⁹ Hence, any endothelial dysfunction, such as denudation via wire injury, inflicts significant vascular abnormalities, as the homeostatic controls are

deregulated. The role that endothelial dysfunction has on smooth muscle cell abnormalities is of specific interest to the development of the neointima, especially when neointimal hyperplasia only ceases when the endothelial layer has regrown.^{9,10}

Subsequently, injury to the top layer of medial VSMCs triggers the activation of vascular smooth muscle cells.¹¹ SMC luminal exposure due to endothelial loss has dramatic effects on the hormonal environment, signal transduction, gene expression and morphology of the vasculature. For example, initial response to injury is known to induce expression of growth factor genes in SMCs, such as PDGF-A and its receptor PDGF- β .¹² Additionally, fibroblast growth factors (FGFs) are released and instigate a medial SMC mitogenic response.¹³ Taken together, the complexity of the pathophysiological response to injury involves a multi-faceted event that combines hormonal alterations, release of circulating factors, expression of adhesion molecules, macrophage activation, and gene expression modifications, which culminate in the transformation of SMCs into a phenotype capable of migration and proliferation into the intima.

Reactive oxygen species

Uncovering the signal transduction pathway of this mechanism has elucidated the identification of a wide variety of molecular players. Central to this pathway, however, are the ubiquitous reactive oxygen species (ROS). ROS are products of oxygen metabolism in all aerobic biological systems. Free radical ROS are categorized as molecules containing one or more unpaired electrons in atomic or molecular orbital.¹⁴ The oxidative state of the cell is an integral homeostatic balance between oxidant and antioxidant cellular components. Consequently, regulatory disturbance of ROS is etiologically significant for numerous diseases, including the development of multiple cardiovascular diseases.^{15,16} The role of ROS in restenosis

was of direct interest due to the demonstrated prevalence of ROS in systemic and cardiac vessels.¹⁷ In the context of restenosis, the demonstration that antioxidant treatment prevents neointima formation unequivocally centers ROS as a mediator in this process.¹⁸ Finally, ROS involvement in the cellular processes of growth, death, and migration of VSMCs and extracellular matrix (ECM) modifications make its pathological production and regulation a vital part of this story.^{19,20}

NADPH oxidase enzymes and ROS production

In VSMCs, ROS, such as $O_2^{\cdot-}$ and H_2O_2 , are derived from the NADPH oxidase (Nox) family of enzymes as well as a wide array of metabolic sources.²¹ Nox enzymes fall into a category of ROS producing enzymes that includes but is not limited to, lipoxygenases, xanthine oxidase, and cytochrome p450.²² The role of Nox in ROS production was first identified in neutrophils when their characteristic instantaneous respiratory bursts were identified as Nox-originating.²³ Moreover, vascular Nox enzymes have been identified to be omnipresent in vascular cells, to have a homeostatic ROS production function, and to differ biochemically from neutrophilic Nox.^{17,20,24} Nox create ROS through a single electron reduction, which begins with the oxidation of NADPH by flavin adenine dinucleotide (FAD) and culminates in the reduction of molecular oxygen to form $O_2^{\cdot-}$ on the surface of the outer membrane.²⁵ Nox characterization as a signal transduction protein is entirely due to its functional capability as a membrane-associated, multi-unit enzyme with multiple regulatory binding domains.^{25,26} Furthermore, the sole functionality of Nox is its ROS producing capabilities.²⁰ Taken together with the Nox-dependent activation of other oxidases in the ROS activation cascade and the importance that ROS has in injury response, the potential central and causative role of Nox in restenosis can not

be underestimated.²⁶ Under normal physiology, low constitutive levels of ROS are an integral part of vascular function.^{17,22,27} However, in the pathological state, Nox located in VSMCs have been proven to produce excess ROS, leading to abnormal growth and migration.^{17,27}

The specific Nox enzymes of interest in the vasculature are Nox1, Nox2, Nox4, and Nox5. The first three are involved in vascular injury response, while the role of Nox5 has not been studied because it is not expressed in rodents, the animal model most widely used to study neointima formation.²⁸ Lee et al. characterized the role of Nox1 in neointima formation following injury, showing that it is involved in VSMC proliferation, migration and matrix secretion.²¹ Nox2 is expressed in endothelial cells of small to mid-sized vessels, but is not found in the VSMCs of large arteries, making it pathologically significant to atherosclerosis and hypertension, but less important in restenosis.²⁶ However, Nox2-derived ROS from inflammatory cells, which infiltrate the vessel wall during injury, should not be ignored as sources of localized ROS during the vascular response. Little is known about Nox5 signal transduction because of its limited species distribution. Lastly, the role of Nox4 in VSMC transformation and restenosis is being uncovered, and research on this protein led to the discovery of the regulatory interaction between Nox4 and polymerase delta interacting protein 2 (Poldip2, also known as PDIP38).²⁹ This study is meant to further elucidate the role of Poldip2 in the injury response.

Polymerase delta-interacting protein (Poldip2)

Lyle et al first identified Poldip2 as a regulator of Nox4 in VSMCs with profound effects on cytoskeletal integrity and cellular migration.²⁹ Nox 4 tissue distribution is widespread and is highly abundant compared to other Nox homologues.²⁵ Nox4 proteins are localized to internal

cellular membranes. The superoxide produced by Nox4 is immediately converted to H_2O_2 ; this is unlike any other form of Nox-derived ROS, and its signaling pathways are believed to be mediated by H_2O_2 .^{25,30} Additionally, Nox4 has a unique constitutive expression characterized by low levels of ROS secretion, and its ROS-producing activity is exclusively dependent on its interaction with the membrane subunit p22phox.³¹ The co-localization of Nox4 and p22phox seems devoid of other cytosolic subunit interactions, which is a hallmark of other Nox homologues.

Pathologically, Nox4 seems to be involved in cell growth, migration, proliferation, death, and differentiation, with some conflicting data.²⁶ Nevertheless, this implies a fundamental role of Nox 4 in a process common to all of these cellular functions. Possible hypotheses for this causative role include gene expression alterations and cytoskeletal reorganization. In fact, *in vivo* and *in vitro* studies have uncovered that Nox4 is related to smooth muscle cell differentiation markers and is necessary for differentiation and re-differentiation, a characteristic plasticity of VSMCs important in vascular development and pathology.^{32,33} Nox4-dependent regulation of differentiation marker genes provides one regulatory role of Nox4 via gene expression control. Furthermore, focal adhesion formation, a necessary cellular pathway for migration of VSMCs, is regulated by Nox4 expression.²⁹ Complicating some of the enigmatic properties of Nox4-derived ROS is the fact that Nox4 H_2O_2 is ubiquitously produced at low levels, and, up until recently, a Nox4 deficient animal model had not been created. This is part of the reason the precise role of Nox4 in neointima formation is still unclear.

As noted, Nox4 does not require the cytosolic subunits used by other Nox enzymes to assemble a functional enzyme. However, recent research has identified Poldip2 as a positive regulator of Nox4. Using a 2-hybrid screen of rat VSMC cDNA, Poldip2 was shown to have an

interaction with the proline-rich region of the p22phox C-terminus, which was identified as a likely binding site for regulatory molecules.²⁹ The interaction of p22phox with Nox1 and Nox4 has been published, and after confirming that Poldip2 unequivocally associates with p22phox through pull-down assays and coimmunoprecipitations, its biological role as a positive regulator of Nox4 was determined.²⁹ Further experiments confirmed Poldip2 expression in tissues rich in Nox4, and its cellular compartmentalization in focal adhesions, stress fibers, and nuclei support the observation that Poldip2 colocalizes with Nox4/p22phox in VSMCs.^{26,29,32}

Very little is known about the polymerase delta-interacting proteins, besides their role as a regulator of cell division and their interaction with DNA polymerase delta and proliferating cell nuclear antigen (PCNA).^{34,35} The localization of Poldip2 to the cytosol and nucleus suggests that it may intrinsically regulate a multitude of cellular functions. The initial discovery of Poldip2 described the protein as a highly conserved DNA polymerase δ -binding partner, which also interacted with PCNA.³⁵ Based on the functional roles of these proteins, it followed suit that Poldip2 should be involved in DNA replication and DNA repair. Furthermore, Klaile et al demonstrated that Poldip2 localization is regulated by an interaction with the homophilic cell-cell adhesion receptor CEACAM1 (carcinoembryonic antigen-related cell adhesion molecule 1) and exhibits an ability to shuttle between nuclear and cytoplasmic compartments in a cell cycle dependent manner.³⁶ Cell adhesion receptors are influential in a multitude of cellular functions that are of interest in neointima formation, including proliferation and gene transcription. The link between Poldip2 and CEACAM1, a modulator of contact-dependent cell survival and growth in epithelial, endothelial, and hematopoietic stem cells, could mean that there exists a novel regulatory interaction between Poldip2 and a similar adhesion molecule in VSMCs, which may potentiate a possible mechanism of Poldip2-dependent cytoskeletal control important in this

process. Moreover, based on its nuclear localization only in proliferating cells, and experiments demonstrating that Poldip2 loss of function results in problematic mitotic spindle organization, irregular chromosome segregation, and multinucleated cells, Poldip2 has a clear function in mediating proper cell division.³⁴ Interestingly, in relation to Nox4, the absence of Poldip2 results in a loss of focal adhesion-localized Nox4, and siPoldip2 cells demonstrate few detectable focal adhesions and a loss of stress fiber tension, whereas Poldip2 overexpression causes focal adhesion elongation and stress fiber thickening.²⁹ Taken together, these data suggest that Poldip2 may regulate the injury response via several mechanisms, some of which may be Nox4 dependent.

Although the complete physiological function of Poldip2 remains elusive, these studies identified the cytoskeleton as a clear target of Poldip2. Its relation to Nox4-dependent focal adhesions, its interaction with cell adhesion molecules, and its regulation of mitotic spindle formation, indicates that it may be linked to a plethora of physiological and pathological processes. The regulation of Nox4 via Poldip2 may also shed light into cellular processes that are known to be affected by Nox-derived ROS, such as proliferation, migration, apoptosis, and cell growth. Especially in pathologies where these cellular processes are dysregulated, targeting Poldip2 expression provides a mechanism for manipulating basal cellular functions related to neointima formation in hopes of uncovering some of the enigmatic properties of Poldip2 and its regulatory interactions. The possibility of a Nox4-independent role for Poldip2 in neointima formation cannot be excluded, however; especially when little is known about this class of proteins, and other research has linked Poldip2 to independent processes that could feasibly turn out to be central mediators in this process.

Aims and hypothesis

Animal models have been used extensively to study the pathology of atherosclerosis and restenosis.^{4,9} In this proposed mouse model of restenosis, a transluminal mechanical wire injury procedure is used to induce neointimal hyperplasia. This method is widely used and effective in producing an injury reminiscent of restenosis. Preliminary studies have shown that heterozygous (Poldip2 +/-) mice that express less functional Poldip2 protein have decreased neointima formation after vascular injury. The purpose of this study is to begin to define the mechanisms by which loss of Poldip2 exerts a protective effect on neointima formation. This project is divided into two main parts. The first aim of this study is focused on defining the characteristics of neointimal ECM in wildtype (WT) and Poldip2 (+/-) mice. The spatial and temporal deposition of the ECM is integral to cellular processes, and could thus be functionally linked to neointima formation. The second aim is dedicated to measuring the rates of apoptosis and proliferation within each animal group, processes that both contribute to neointimal thickening. Apoptosis rates are easily measured using TUNEL labeling. However, it became a necessary part of this aim to develop and optimize a method for proliferation assessment using proliferating cell nuclear antigen (PCNA) immunolabeling. Understanding the dynamic relationship between the cellular response to stress and intrinsic matrix composition will provide insight into how Poldip2 (and potentially Nox4) contribute to vascular disease. We hypothesize that a reduction in neointima formation in Poldip2 (+/-) mice compared to WT mice is associated with abnormal collagen deposition and decreased vascular smooth muscle cell proliferation, but no change in apoptosis.

MATERIALS AND METHODS

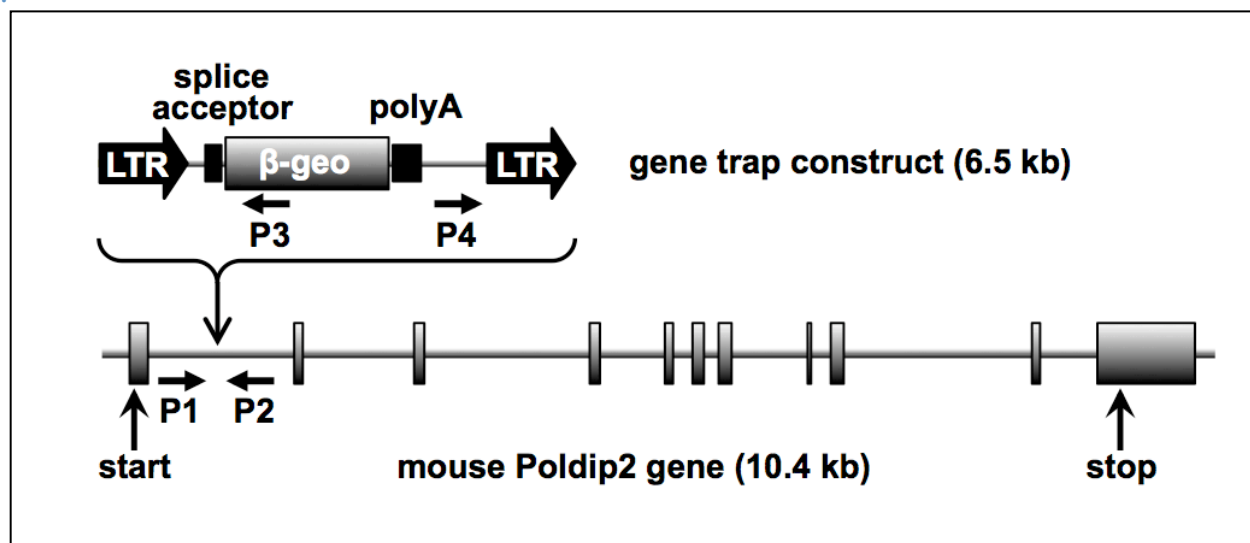


Figure 2- Interruption of the Poldip2 gene at intron 1. Courtesy of Bernard Lassègue, PhD.

Animals

Poldip2 gene trap mice were generated from a clone (IST12080D9) of C57BL/6N embryonic stem cells with a gene trap insertion in the first intron of the Poldip2 gene (Texas A&M Institute for Genomic Medicine, College Station, TX) (Figure 2). Through high throughput methods with insertion of the gene-trapping vector VICTR76, selection by neomycin resistance, and insertion site genome identification, the gene trap stem cells were identified, injected into blastocysts and implanted into albino pseudopregnant mice. A Poldip2 (+/-) mouse lineage was established when high percentage chimeras were crossed with C57BL/6 mice. C57BL/6 mice wildtype (WT) for Poldip2 were used as controls. It should be noted that the complete loss of Poldip2 expression is embryonically lethal; hence, a Poldip2 knock out model was not feasible. The heterozygotes, nevertheless, contain one nonfunctional copy of the gene, which is enough to induce a functional reduction in the gene's expression.

Transluminal mechanical injury

All procedural protocols followed the guidelines set forth by the Emory University Institutional Animal Care and Use Committee. Surgeries were performed on mice 4-6 months old within each experimental group. Mice were anesthetized by intraperitoneal injection of 10 mg/kg xylazine, and 80 mg/kg ketamine diluted in 0.9% sodium chloride solution.²¹ To induce restenosis, a transluminal mechanical injury was performed on the left bilateral femoral artery. The femoral artery was accessed via blunt dissection, and blood flow was controlled via proximal and distal suture tourniquet application. A large wire (0.38-mm in diameter) was inserted into the left femoral artery toward the iliac artery and left in place for approximately a minute to denude and dilate the artery, as previously described.²¹ The wire was removed, and blood flow was returned to the artery. Animals were returned to the vivarium until euthanasia at the appropriate time points (Figure 3). All surgeries were performed by Dr. Srinivasa Raju Datla.

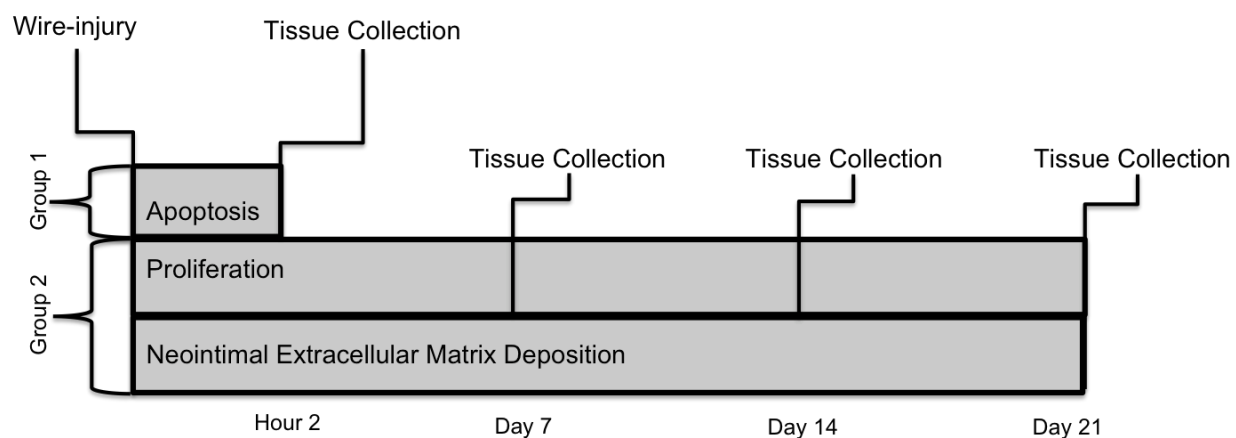


Figure 3- Timeline of femoral artery collection. VSMC apoptotic rates were measured two hours after transluminal wire injury. Neointimal extracellular matrix deposition was only measurable at day 21-post surgery, when neointimal collagen deposition was observable. VSMC proliferation was quantified at day 7, day 14, and day 21-post surgery.

Tissue collection and slide preparation

All animals were euthanized by CO₂ inhalation. To assess apoptosis, Group 1 (n=4 WT, n=4 Poldip2 +/-) animals were euthanized two hours post surgery, pressure-perfused with a 100 mm Hg with 0.9% sodium chloride solution and pressure-fixed with a 4% paraformaldehyde solution. The affected length of the injured arteries was excised and embedded in paraffin. Contralateral uninjured femoral arteries were collected as controls for all animals. Serial cross sections were cut in 7 µm thicknesses with a RM 2235 Microtome (Leica).

For studies on ECM composition and proliferation, Group 2 animals were divided into three cohorts, day 7 (cohort A, n=5 WT, n=5 Poldip2+/-), day 14 (cohort B, n=3 WT, n=3 Poldip2 +/-), and day 21 (cohort C, n=4 WT, n=4 Poldip2+/-). Animals were euthanized and flushed with a 0.9% sodium chloride saline solution. Injured and uninjured arteries were excised and independently placed in Tissue-Tek[®] OTC (Sakura) compound on liquid nitrogen for rapid cooling and hardening of the storage compound. All blocks were stored at -80°C until cryostat section cutting. Serial femoral cross sections of 7 µm thickness were cut using a CM3050 cryostat (Leica) at -21°C chamber temperature. Cross sections were labeled and stored at -80°C until staining or immunolabeling. Frozen sections were chosen instead of paraffin sections to prevent the possibility that tissue fixation and processing may denature some of the antigens of interest.³⁷

Collagen staining

To assess collagen deposition, a picrosirius red collagen stain was used. Selected slides from each group 2 cohort were subjected to the same experimental conditions. The cross sections were air dried for 30 minutes, fixed and permeabilized in acetone for 5 minutes, and air-dried

again for 10 minutes. After rehydration in phosphate buffered saline (PBS), a haematoxylin (Thermo Fisher Scientific) counterstain was applied for 8 minutes and then washed in running tap water. Cross sections were then stained in a picosirius red solution (0.001 g/ml Direct Red 80 in saturated aqueous picric acid) (Sigma- Aldrich) for an hour. After washing in acidified water, the slides were mounted in cytooseal 60 (Thermo Fisher Scientific).

Apoptosis

Paraffin embedded cross sections were deparaffinized in changes of xylene and hydrated in the appropriate graded alcohol concentrations. Serial sections were stained with haematoxylin and eosin to assess the integrity of the injured arteries post surgery. The *in situ* cell death detecting kit, TMR red (Roche) was used to visualize apoptotic cells. Slides were similarly deparaffinized and hydrated and then irradiated at 750W for 1 minute in 0.1 M citrate buffer, pH 6.0. Following a 30-minute blocking at room temperature in 0.1 M Tris-HCl, 3% bovine serum albumin (BSA), and 20% fetal bovine serum at pH 7, selected slides were subjected to the TUNEL reaction mixture containing the terminal transferase for an hour. Incubation with recombinant RNase free DNase I for 10 minutes prior to labeling with the TUNEL reaction mixture was used as the positive control. Labeling solution without the terminal transferase was used for the negative control. Slides were rinsed in PBS and mounted with mounting media with DAPI for fluorescent microscopy (Vector Labs).

Proliferation detected by immunofluorescent histology

Frozen slides were selected from each cohort of group 2. They were air dried for 30 minutes and fixed in 3.7% formaldehyde in 0.2M Tris-buffered saline (TBS), pH 7.6, for 5

minutes at room temperature (RT), followed by an extra 5 minute fixation step at RT with a Carnoy's solution (6:3:1 ethanol, chloroform, acetic acid by volume).³⁸ Once fixed, the slides were dried for an additional 10 minutes. After rehydration in PBS, tissues were carefully permeabilized with 0.1% triton X-100 in PBS for exactly 5 minutes. Following vigorous washing in PBS, endogenous activity was blocked with 2% BSA, 2% normal donkey serum in PBS (Vector Labs) for an hour. Immediately following blocking, slides were incubated with the rabbit polyclonal anti-PCNA primary antibody in blocking buffer at 4°C overnight (Abcam, 1:500). The secondary Alexa Fluor[®] 568 donkey anti-rabbit antibody was diluted in blocking solution and applied for 30 minutes following washing of the primary with PBS (Vector Labs, 1:200). Slides were rinsed in PBS and mounted with mounting media with DAPI (Vector Labs). For negative controls in each experiment, incubation with the primary antibody (PCNA) was excluded.

Vascular smooth muscle cell identification with alpha-actin immunofluorescent histology

Representative slides from each cohort were fixed, hydrated, and blocked following the same procedure as described. A rabbit polyclonal anti-SMC α -actin (Abcam, 1:400 working dilution) was applied for 2 hours. An Alexa Fluor[®] 568 anti-rabbit secondary (Invitrogen, 1:200 working dilution) was applied for 30 minutes, and the same mounting media containing DAPI was used for nuclear staining (Vector Labs).

In vitro studies

For *in vitro* studies conducted by Dr. Srinivasa Raju Datla, VSMCs were isolated from mouse thoracic aortas by enzymatic digestion. Aortas were excised, cut, cleaned, and digested

with the digestive enzymes, collagenase and elastase. Dissociated VSMCs were plated and grown in Dulbecco's modified Eagle's medium (DMEM) containing 10% fetal bovine serum, 100 U/ml penicillin, and 100 µg/ml streptomycin. VSMCs were either treated with stealth siRNA for Poldip2 (Invitrogen) or a stealth control siRNA (siControl), for baseline comparisons (Invitrogen). To determine the extent of VSMC ECM protein production in each cell treatment, VSMCs lysates were immunoblotted for collagen I and fibronectin. All results were measured via western blot band intensity quantification. To analyze proliferation, siPoldip2 treated VSMCs and siControl treated VSMCs were plated at the same density on a 35 mm dish, and starved in serum-free media. Proliferation was induced at day 0 with the addition of serum, and cell number counts were obtained up to day 6. Cell counts in each treatment group were done with a Neubauer hemocytometer (Fisher Scientific).

Microscopy

All cross sections were mounted on cover slips with the previously described mounting media (Vector Laboratories and Thermo Fisher Scientific). Images were acquired with an Axioskop microscope and Axiocam CCD camera (Carl Zeiss Inc). Images for each experiment were taken in one sitting to minimize any aberrations in optical conditions. This was especially crucial while visualizing collagen under polarized light, as background light can disrupt the capture of the birefringent fibers. Images of each injured and uninjured artery were taken at 20x and 40x magnification. Representative images were also taken at 10x magnification.

Image analysis and calculations

Collagen deposition- Images were uploaded into ImageJ software (NIH). Images were split according to color channels to match birefringence color. The areas of interest (AOIs) were selected prior to gray scaling to delineate the neointima from the external lamina. The background of each image was subtracted and a constant threshold min/max was applied across all images to measure the birefringence using a binary black and white image. Selected areas were converted from pixels to μm^2 based on reported pixel/ μm ratios at each magnification (Carl Zeiss Inc). The amount of collagen deposition was calculated as the ratio of collagen area to neointima area.

Apoptotic medial VSMCs- Images were uploaded into Image Pro Plus (IPP), image processing, enhancement and analysis software (Media Cybernetics). Apoptotic cells were calculated based on the observed count of TUNEL-DAPI positive cells within the AOIs. Apoptosis is shown as the quotient of $(\text{TUNEL-DAPI}^+_{\text{cells}})/(\text{Total Cell Count})$ multiplied by 100. As a control, the number of cells present within each medial layer of all experimental groups was also calculated.

Proliferating VSMCs- Images were uploaded into Image Pro Plus (IPP). The number of proliferating cells was determined based on the observed count of PCNA positive nuclei counterstained with the nuclear stain, DAPI, within the AOIs. Percent proliferation is shown as the quotient of $(\text{PCNA-DAPI}^+_{\text{cell}})/(\text{Total Cell Count})$ multiplied by 100.

Statistical analysis

Results are shown as mean \pm SEM. Statistical analysis was carried out using GraphPad Prism software. Statistical significance was determined using appropriate unpaired t-test, and

one-way, and two-way ANOVA measurements with post-hoc tests using confidence intervals of 95%. A probability value of <0.05 was considered significant.

Statement of authenticity

Unless otherwise noted, all experiments performed for this thesis were conducted by the author, Mark Harousseau.

RESULTS

Poldip2 (+/-) heterozygosity and neointimal reduction

Previous experiments conducted in Dr. Griendling's lab used amplification of the strain's genomic DNA with a standard three primer PCR to confirm the recombination of the Poldip2 gene in live mice. The transcription of the recombinant gene is predicted to end after the poly-A tail present in the recombinant construct, eliminating Poldip2 gene transcription (Figure 2, courtesy of Bernard Lassègue). After confirmation of the successful interruption of the Poldip2 gene, the three primers P1, P2, and P4 were used to confirm the genotype of all the mice used in these experiments.

Initial femoral artery transluminal wire injuries conducted by Srinivasa Raju Datla were used to characterize the heterozygotes response to transluminal femoral wire injury. As shown in Figure 4, Poldip2 (+/-) mice demonstrate a significant decrease in neointimal luminal protrusion three weeks post wire injury with respective controls shown ($P < 0.05$). H&E staining was used to visualize the vessel for morphometric analysis of the percent stenosis within the vessel cross-sections (Figure 5). Heterozygous mice demonstrate a less pronounced neointima, which can be observed by less prominent luminal stenosis. Measurements were taken as the ratio of intima to media layer area to account for any variation in arterial morphology between animals. Taken together, these data show that loss of Poldip2 attenuates the response to injury. There are multiple possible and plausible mechanisms by which this gene trap model could result in this less drastic pathology, two of which are extracellular matrix deposition and VSMC growth/death.

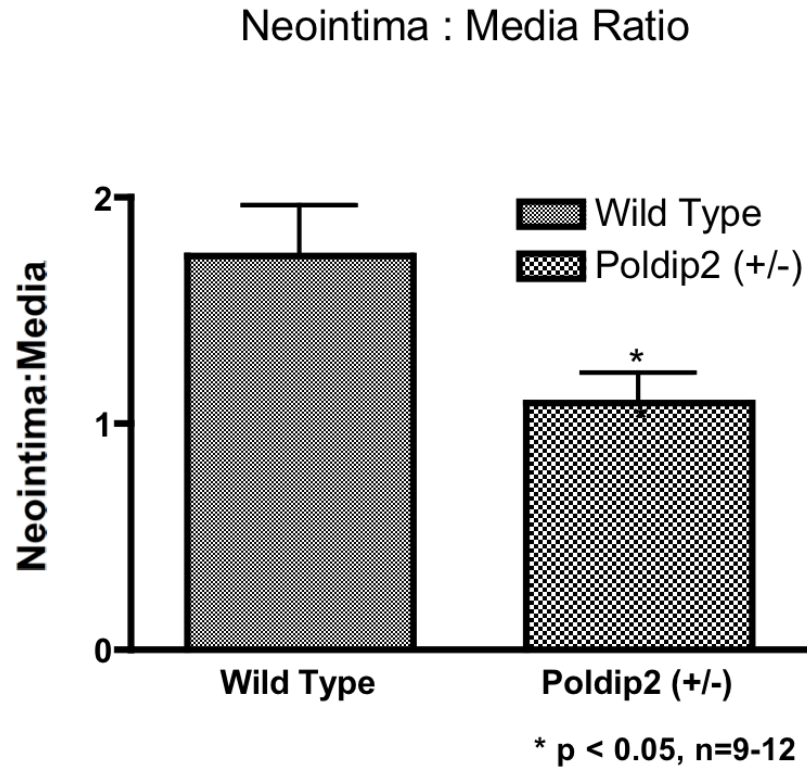


Figure 4 The ratio of intima to media layer areas. Courtesy of Srinivasa Raju Datla, unpublished data. Animals were euthanized three weeks post wire injury. Neointima formation was assessed using H&E staining (Figure 4). The difference in arterial structure was measured as the ratio of intima to media. Statistical significance: * $P < 0.05$ (t-test).

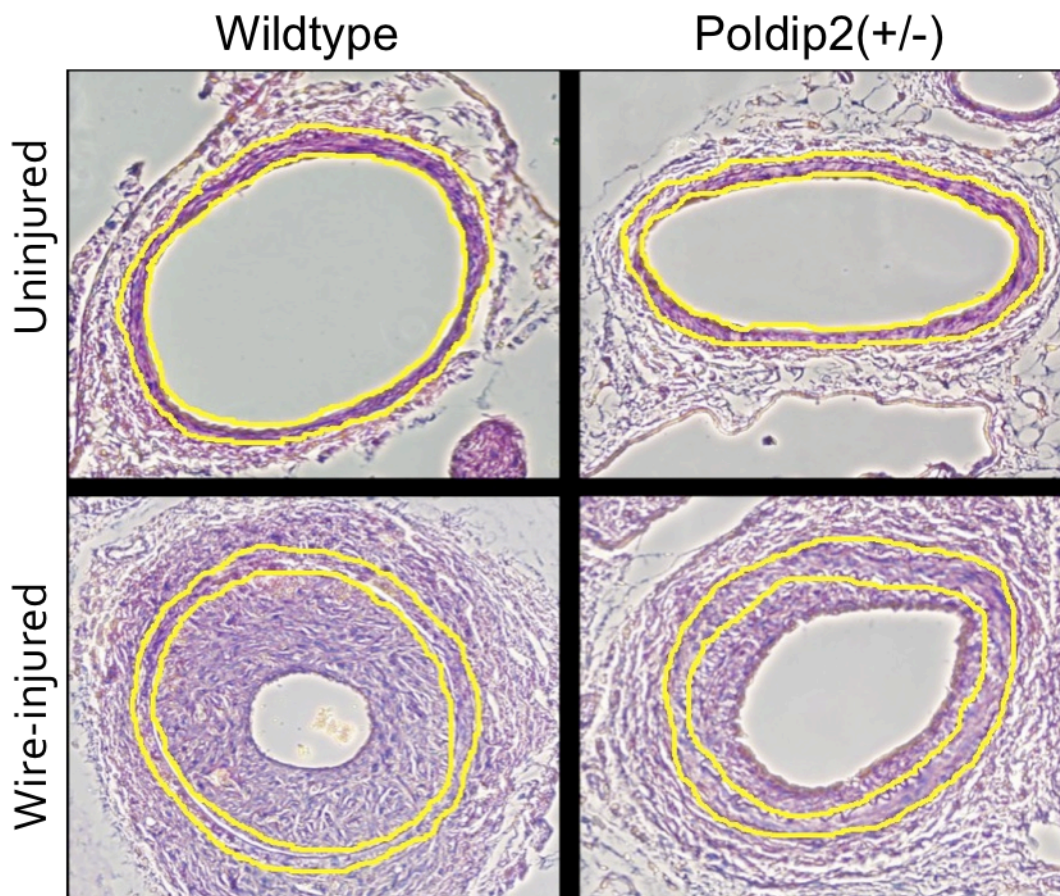


Figure 5- Haematoxylin and Eosin staining of wildtype and Poldip2 (+/-) uninjured and wire-injured femoral arteries. Courtesy of Srinivasa Raju Datla, PhD, unpublished data. Poldip2(+/-) animals demonstrate less neointimal formation, observed by a greater luminal/neointima area. The internal and external laminae are outlined in yellow, delineating the medial layer from the neointima.

In vitro VSMC secretion of ECM components

An experiment conducted by Dr. Srinivasa Raju Datla assessed the secretion of ECM protein components in VSMCs treated with stealth siRNA for Poldip2 (Invitrogen). A stealth control siRNA (siControl) was used for baseline comparisons (Invitrogen). The results, as measured via western blot analysis, show that both collagen I and fibronectin, the main protein components of ECM, increase when Poldip2 translation is decreased by siRNA treatment (Figure 6). To control for variations in cell growth rate, which may affect ECM production, the gels were

adjusted for total protein concentration. These results indicate that loss of Poldip2 increases matrix production, suggesting that Poldip2 may normally inhibit ECM secretion.

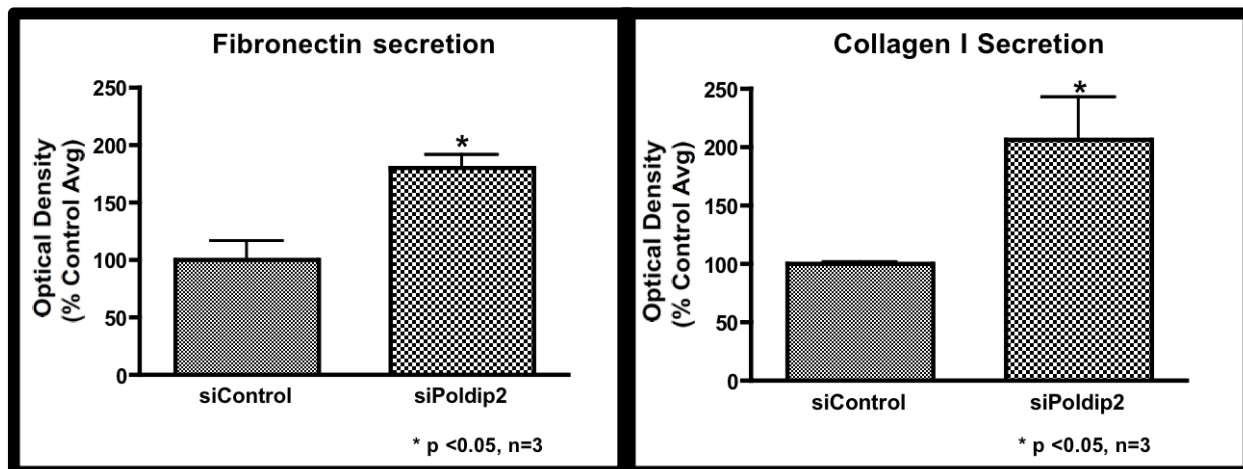


Figure 6- *In vitro* ECM protein production. Courtesy of Srinivasa Raju Datla, PhD, unpublished data. Treatment of aortic smooth muscle cells with siPoldip2 increases Fibronectin and Collagen I secretion. Statistical significance: * $P < 0.05$ (t-test).

In vivo characterization of collagen

To determine whether or not the *in vitro* studies were of significance *in vivo*, picrosirius red staining for collagens I-III was used to determine the extent of collagen deposition within the neointima 21 days post wire injury in both WT and Poldip2 (+/-). Upon initial observation, it became clear that the only collagen fiber observable within the neointima was the red/orange birefringence of thicker, more established fibers.³⁹ Within the adventitia, which is not of direct relevance to the injury response, a color range of orange/red, and green birefringence was observed (data not shown). Green birefringence indicates thinner, more recently generated collagen and sometimes fibrin fibers.⁴⁰

Each artery was observed under brightfield and circular polarized light (Figure 6). Images taken at 20x magnification were used for measurements. After generation of the binary black and white 8-bit gray scale from the red channel, the same threshold was applied across all sections

(Figure 8). Since the only hue present, in small amounts, was red, RGB channeling was split to account for only the red birefringent hue. This circumnavigated the issues that have been reported with picosirius red staining fibrin fibers, and selectively identified collagen fibers.⁴⁰ Consistent with the cell culture data, calculations indicate that Poldip2 (+/-) mice deposit more collagen within the neointima 21 days post wire injury than WT mice. There was a three-fold increase in collagen birefringence in Poldip2 (+/-) neointima compared to WT neointima, with a significant *P* value of 0.016 (Figure 8). Neointimal collagen birefringence was not significantly pronounced at day 7 and day 14, making neointimal measurements practically impossible at those time points.

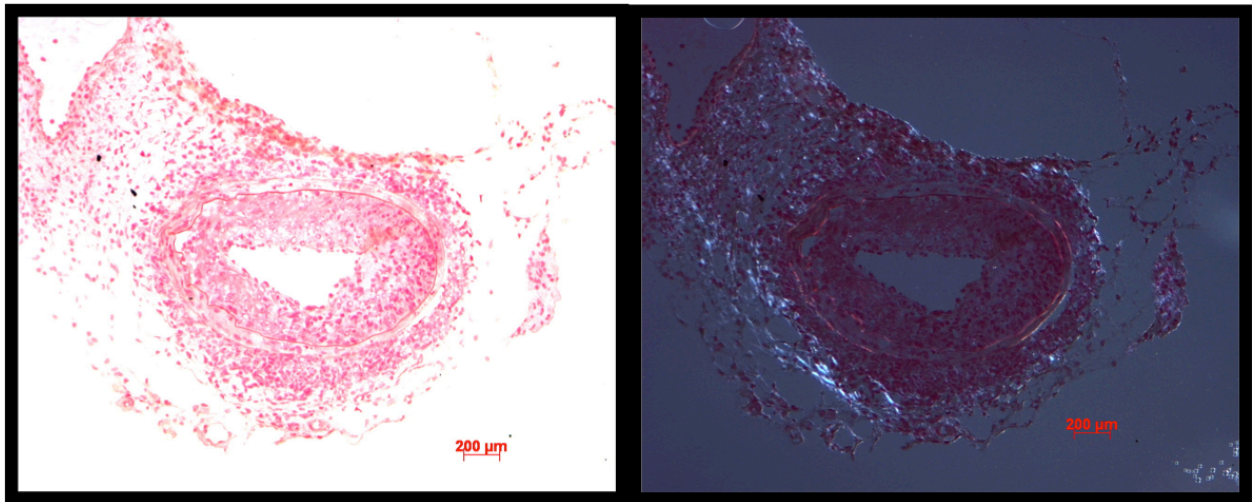


Figure 7- Picosirius Red Stain for Collagen. The image on the left is the artery under brightfield microscopy. The image on the right is the artery under circular polarized light microscopy. The adventitia and the elastic laminae demonstrate the strongest birefringence.

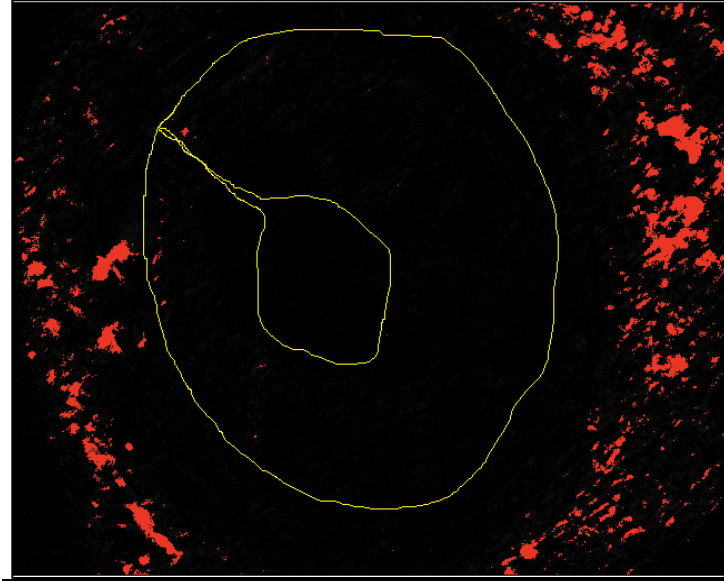


Figure 8- Collagen deposition measurement in the neointima using ImageJ Software. With the background subtracted, the red color channel selected and converted to a gray scale, the threshold was set the same for all arteries, and collagen areas were measured in each areas of interest (AOIs) (μm^2).

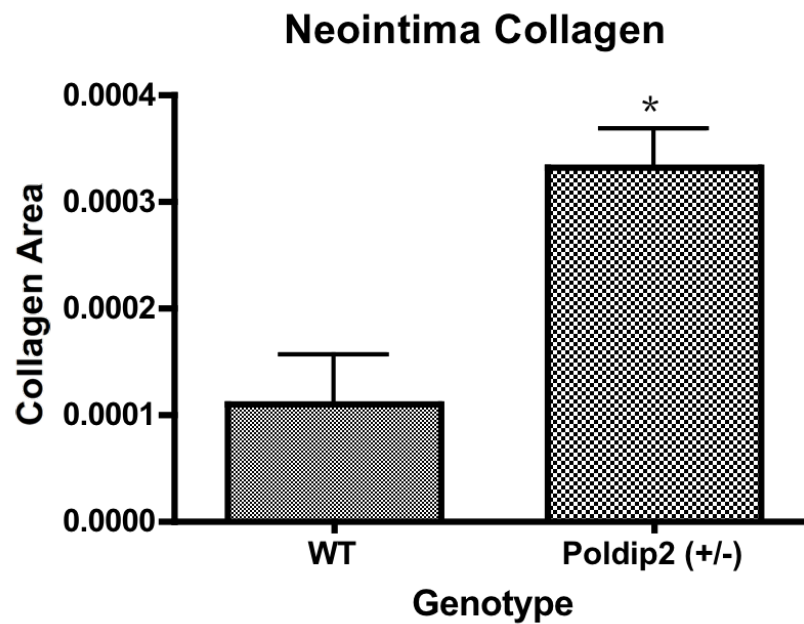


Figure 9- Collagen deposition in the neointima. Measurements were taken using Image J software. Collagen area is shown as the ratio of the birefringent collagen to the area of the neointima. Statistical significance: $P < 0.05$ (t-test)

Medial layer apoptosis

Transluminal wire injury is known to induce rapid apoptosis of medial layer cells, which can then release cytokines and ROS that enhance the growth and migration of the remaining cells.¹⁰ Injured and uninjured femoral arteries were collected from each mouse two hours post surgery and subjected to TUNEL labeling to detect apoptosis after the integrity of each artery was confirmed with haematoxylin and eosin staining (data not shown). A positive control using an RNase-free DNase incubation step prior to TUNEL labeling was performed on uninjured cross sections, which clearly localized the fluorescent tag to the nucleus (Figure 10).

Additionally, the total number of cells present within each medial layer was measured (Figure 11). There was no significant difference in the amount of cells present across all cross sections used.

Just two hours post wire injury, the onset of pathological stimulus can be visualized in both animal groups. In fact, the natural autofluorescence of the vessel wall is accentuated in the injured arteries, presumably due to the natural inflammation of the innate immune response to injury (Figure 10). Apoptotic cells localized to the medial layer were considered for this study. Nuclei stained with DAPI were used as nuclear markers, and a pure blue fluorescence was considered non-apoptotic. The percentage of medial TMR Red-DAPI+ cells is shown in Figure 11. The percentage of apoptotic cells remained the same between Poldip2 (+/-) and WT animals with no significant difference (Figure 11). Uninjured arteries showed no sign of apoptosis, as expected.

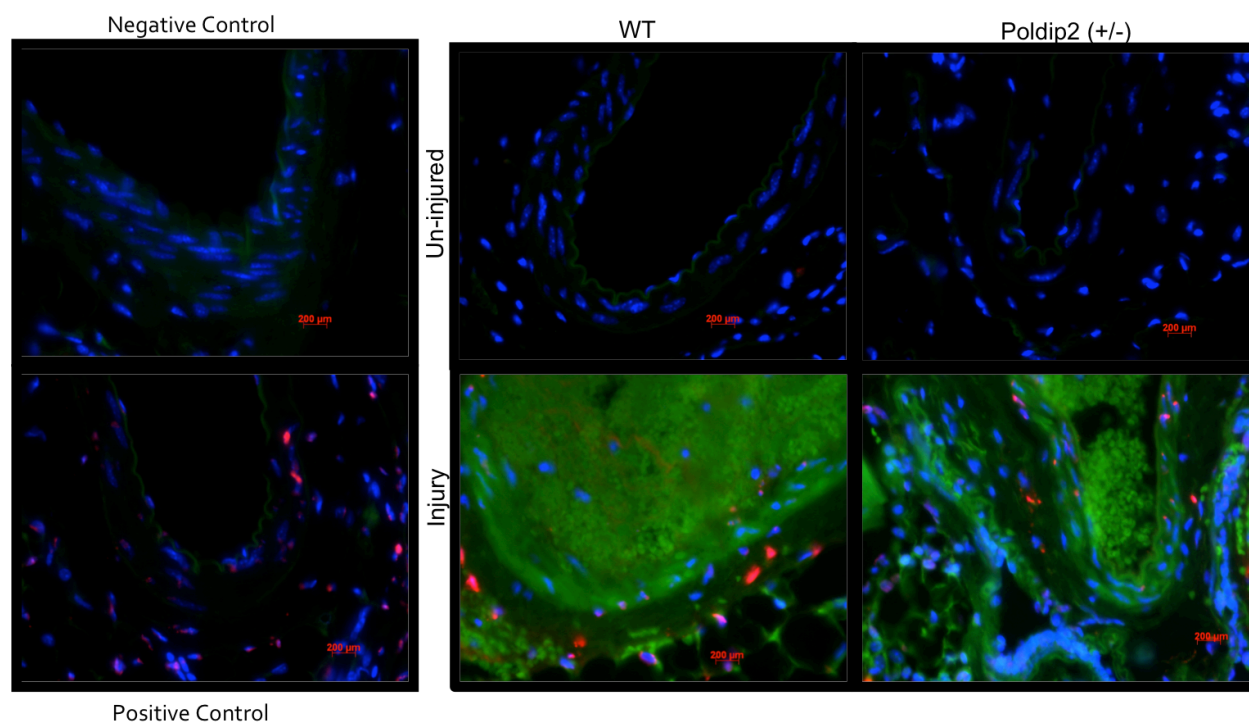


Figure 10-Medial layer apoptosis two hours post wire-injury. Appropriate controls are on the left. An RNase Free DNase incubation step was added as the positive control. Apoptotic cells are labeled red and non-apoptotic cells are labeled blue. Femoral arteries autofluoresce green.

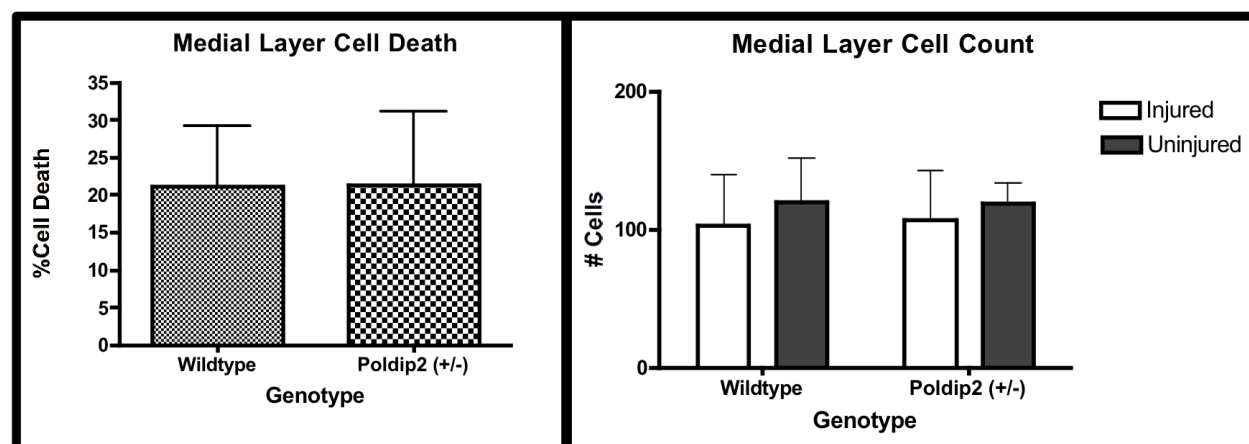


Figure 11- Poldip2 has no effect on medial layer cell death. The percentage of TMR Red cells DAPI+ are shown. The number of cells present within each medial layer was measured to make sure adjustments were not needed for cellular density variations. $P > 0.05$

In vitro siPoldip2 limits proliferation

Experiments conducted by Dr. Srinivasa Raju Datla *in vitro* demonstrate that VSMCs treated with siPoldip2 proliferate to a lesser extent than VSMCs treated with siControl (Invitrogen) (Figure 12). Growth was induced with the addition of serum at day 0, and cell growth was measured at each time point. As seen in Figure 11, siPoldip2 treated cells express a lower growth rate curve, which can be attributed to a decrease in proliferation. The exact mechanism by which this occurs is currently being studied in Dr. Griendling's Lab

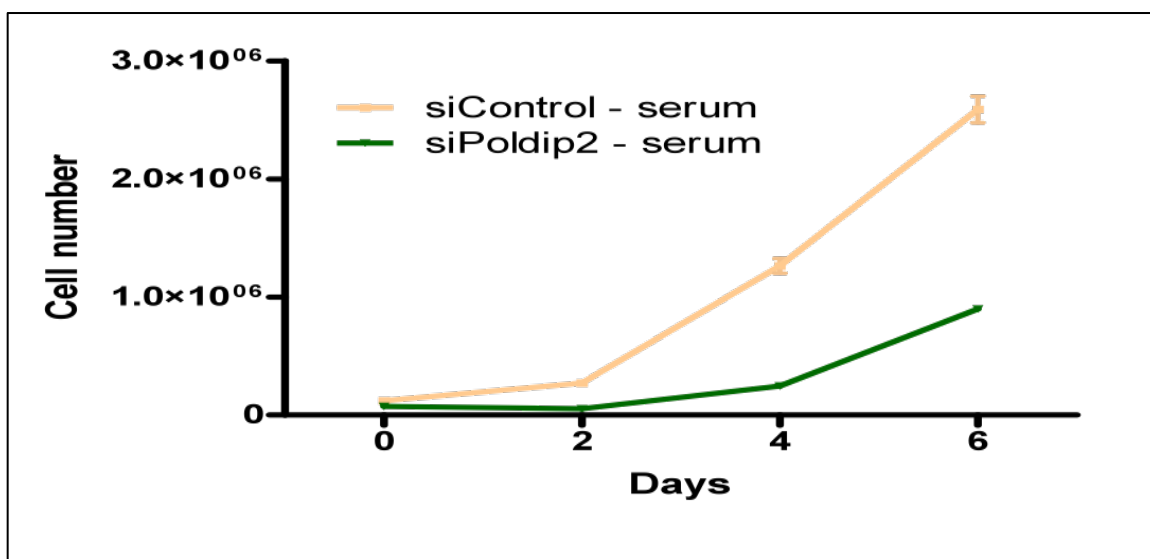


Figure 12- siPoldip2 treatment inhibits smooth muscle cell proliferation. Courtesy of Srinivasa Raju Datla, PhD, unpublished data. siPoldip2 cell number counts were significantly different than siControl cell number counts.

Optimizing PCNA Immunolabelling

Injured femoral arteries were immunolabeled for PCNA (proliferating cell nuclear antigen) to assess proliferation within the media and neointima. In the nucleus, PCNA is a replication factor associated with DNA polymerase δ expressed during S phase. The immunoreactivity of PCNA on paraffin embedded sections has been well documented and yields

strong labeling.³⁸ Successful cryostat immunolabeling is more complicated and correct fixation to access the specific epitope is widely discussed in the literature, often with differing observations.^{38,41,42} Standardizations for this method were carried out on arteries collected two weeks post wire injury, as preliminary studies suggested that this time point may coincide with maximum cell proliferation.

Initial experiments using a primary antibody against PCNA raised in mice yielded strong background staining making quantification of a nuclear signal impossible (data not shown). A rabbit polyclonal anti-PCNA antibody was used for all of the following troubleshooting methods, with representative images shown in Figure 13. The first experiments used acetone as the fixating agent as recommended by the antibody provider for IHC cryostat experiments (Abcam). As seen in Figure 13 (A-B), strong background staining present in both injured (A) and uninjured (B) arteries indicated that additional troubleshooting was necessary. A three-step avidin-biotin complex method with alkaline phosphatase as the substrate was applied to increase the sensitivity of the labeling as performed in Lee et al.²¹ Primary antibody dilutions of 1:50, 1:100, 1:200, and 1:500 were all tested, and yielded similar nonspecific cytoplasmic staining. Primary antibody working dilutions 1:500 were subsequently used to conserve antibody usage. TBS, instead of the commonly used PBS, was used as the buffer solution in all washing and incubation steps due to phosphate inhibition of alkaline phosphatase activity, which is necessary for the final Vector[®]Red color reaction. Although negative controls lacked any staining, uninjured tissues demonstrated strong color labeling, which is not expected as VSMCs in these vessels are differentiated and non-proliferative (Figure 13D). Although some nuclear labeling pattern can be seen (Figure 13C), expansion of this method across cohorts made it clear quantification would be practically impossible, especially knowing that addition of a nuclear counterstain, such as

haematoxylin, would, although necessary, further complicate the issue. With some reports calling for formaldehyde fixation for strong nuclear signal, a supplemental standard using this fixation agent instead of acetone was used to no avail. Another experiment conducted by Giji Joesph using a Qdot[®] Antibody Conjugation Kit with dilutions of 1:500 and 1:1000 yielded similar non-nuclear cytoplasmic staining (data not shown).

A study conducted by Baum et al addressed some of the fixation requirements necessary for the immunoreactivity of PCNA antibody on cryostat sections.^{21,38} A Carnoy's solution, which reportedly yields faint background staining, was used for an additional five-minute fixation step following the initial fixation with 3.7% formaldehyde. The standard included two primary antibody working-dilutions of 1:500 (Figure 13G and 13H) and 1:1000 (Figure 13E and 13F). The latter dilution eliminated almost all of the background staining in the uninjured section (Figure 13G) and made quantification of the nuclear-localized PCNA+ cells possible (Figure 13E). The IgG control demonstrated no nuclear immunolabeling. This method adequately limited most background staining and yielded strong labeling of proliferating nuclei, enabling clear quantification in IPP.

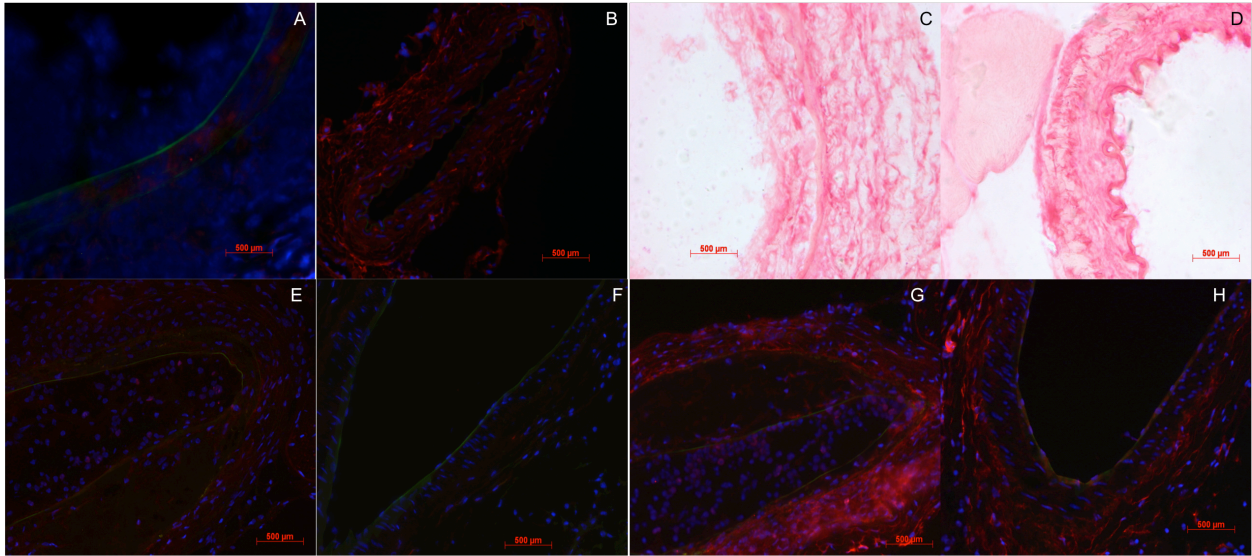


Figure 13- Optimization of PCNA immunolabeling. (A-B) Wire-injured (A) and uninjured (B) immunofluorescently labeled femoral arteries with an acetone fixation step. (C-D) Immunolabeling using a three-step ABC method with alkaline phosphatase as the colorimetric substrate. (E-F) Arteries fixed in 3.7% formaldehyde and Carnoy's solution with a primary antibody dilution of 1:500. (G-H) Arteries fixed in 3.7% formaldehyde and Carnoy's solution with a primary antibody dilution of 1:1000.

Proliferation within the medial layer and neointima following wire injury

The aforementioned protocol was carried out on collected slides from each cohort, using the same exact conditions. Representative images from both animal groups are shown in Figures 14-16. At each time point, the percent of proliferating cells was calculated within the medial layer and the neointima. Trends are shown in Figure 17. At one-week post injury, 13.4% and 11.7% of cells in the neointima were proliferating in WT and Poldip2 (+/-), respectively ($P>0.05$). Within the medial layer, percent proliferation was two-folds greater in WT medial layers compared to Poldip2 (+/-) medial layers, with respective values of 11.9% and 5.2% ($P>0.05$). At two weeks post injury, proliferation in the neointima was 15.3% in WT and 19.1% in Poldip2 (+/-) ($P>0.05$). Medial layer proliferation peaked at 31.4% and 15.3% in WT and Poldip2 (+/-) arteries, respectively ($P>0.05$). Lastly, no proliferation was observed in Poldip2 (+/-) neointima and medial layers three weeks post injury, and in WT animals, 0.8% and 0.9% of

cells were proliferating in the neointima and medial layer, respectively. Within the neointima, this drop in proliferation was significant in both WT ($P<0.01$) and Poldip2 (+/-) ($P<0.05$) groups. In the medial layer, the drop in proliferation was only significant for the Poldip2 (+/-) group.

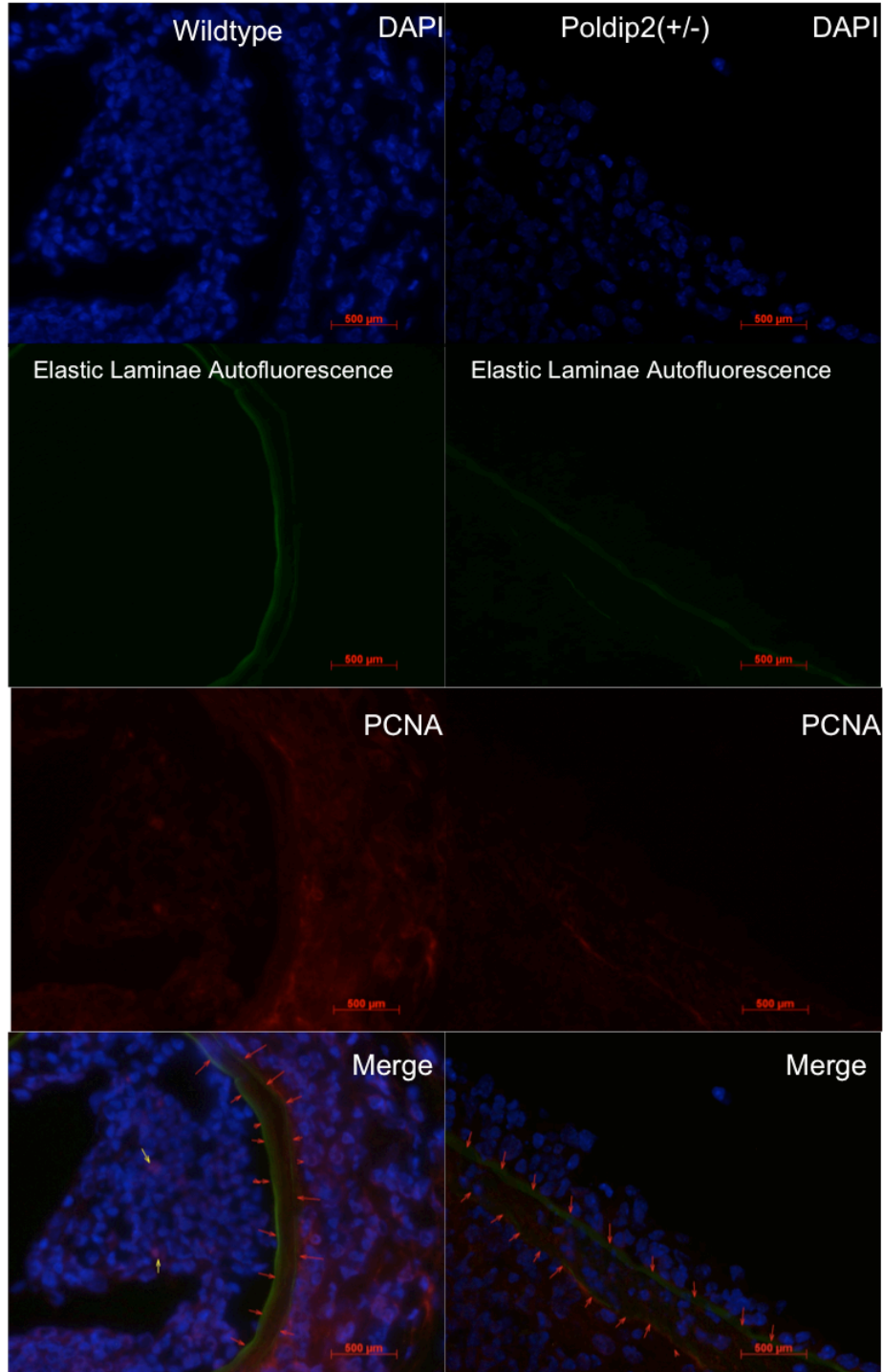


Figure 14- Proliferation one week post wire injury as assessed by immunofluorescent labeling for PCNA. A representative wildtype wire-injured femoral artery is shown on the left. A representative Poldip2(+/-) wire-injured femoral artery is shown on the right. Red arrows in the merged images represent the medial layer, and yellow arrows represent nuclei positively labeled for DAPI and PCNA.

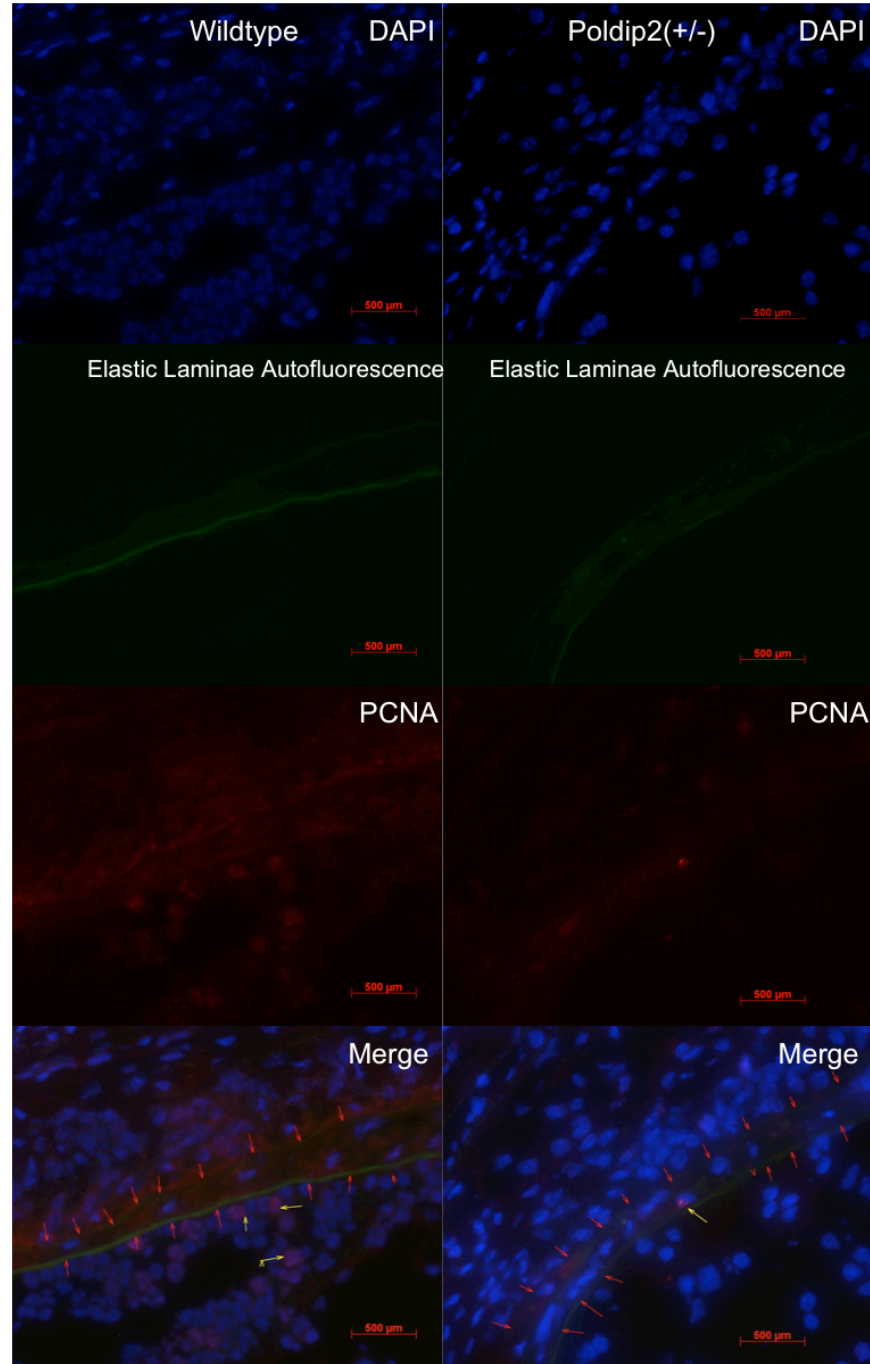


Figure 15-Proliferation two weeks post wire injury as assessed by immunofluorescent labeling for PCNA. A representative wildtype wire-injured femoral artery is shown on the left. A representative Poldip2(+/-) wire-injured femoral artery is shown on the right. Red arrows in the merged images represent the medial layer, and yellow arrows represent nuclei positively labeled for DAPI and PCNA.

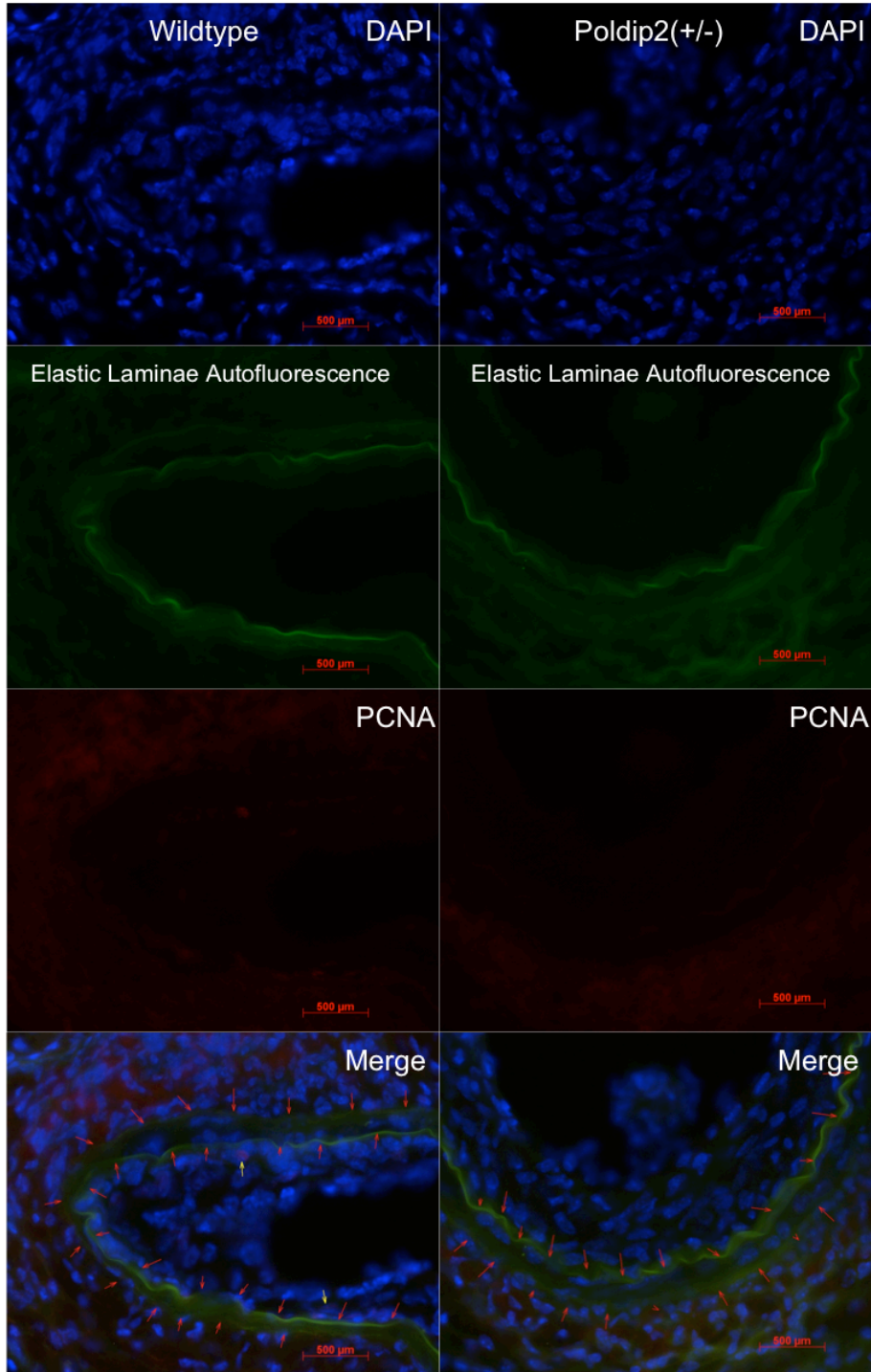


Figure 16- Proliferation three weeks post wire injury as assessed by immunofluorescent labeling for PCNA. A representative wildtype wire-injured femoral artery is shown on the left. A representative Poldip2(+/-) wire-injured femoral artery is shown on the right. Red arrows in the merged images represent the medial layer, and yellow arrows represent nuclei positively labeled for DAPI and PCNA.

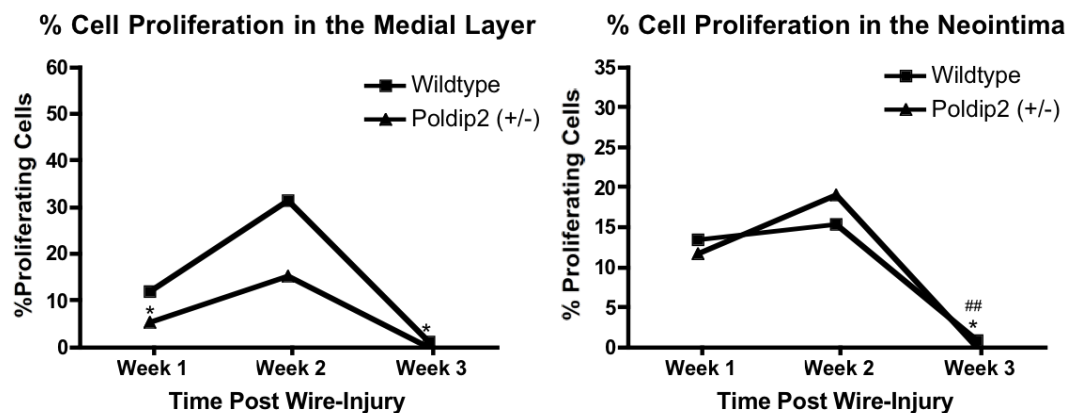


Figure 17- Percent proliferation within the neointima and medial layers of both animal groups. Significant values: * $P < 0.05$ (Poldip2^{+/-}, one-way ANOVA followed by Newman-Keuls Multiple Comparison Test), ## $P < 0.01$ (WT, one-way ANOVA followed by Newman-Keuls Multiple Comparison Test).

Cellular counts within the medial layer and neointima

Total cell counts were calculated within all AOIs for both animal groups and results are shown in Figure 17. There was no statistical difference in medial layer cell counts across all time points. Within the WT neointima, each successive time point demonstrated an increase in the number of cells. A similar trend was observed in Poldip2 (+/-), but to a lesser extent. A significant difference between the number of cells present in the neointima between each genotype was not observed until week 3, where there is a pronounced increase in the amount

cells present in the WT neointima ($P<0.01$).

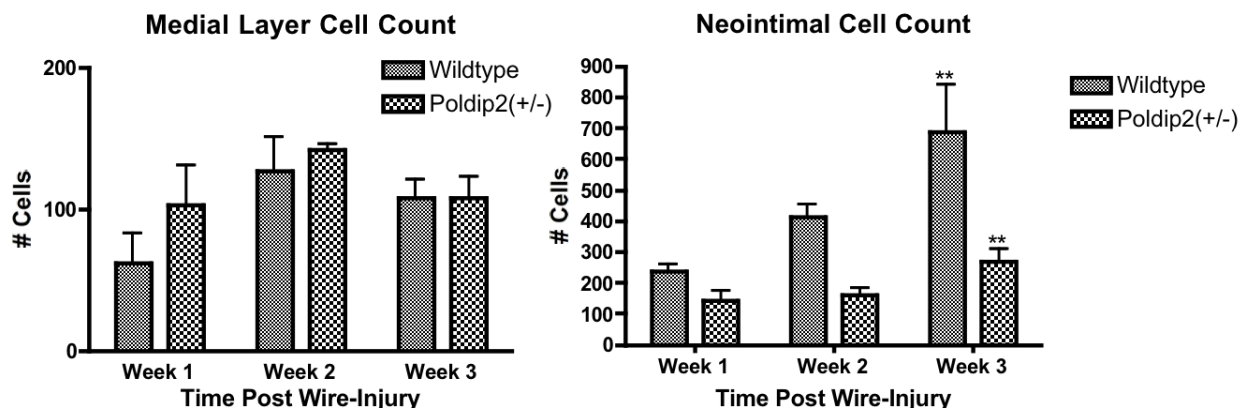


Figure 18- Cellular counts within the AOIs of each animal group. Statistical significance: ** $P<0.01$ (two-way ANOVA with Bonferroni post-tests).

Vascular smooth muscle cell localization

Smooth muscle α -actin immunolabeling of selected arteries was performed to confirm that VSMCs are the majority cell type in the neointima, as inflammatory cells and fibroblasts can also be detected under some circumstances. The results are shown in Figure 19. Arteries from each animal group were selected and incubated with rabbit polyclonal anti-SMC α -actin to specify smooth muscle cell localization. Observations showed little to no labeling in the adventitia, and ubiquitous labeling in the medial layer and neointima three weeks post injury. An IgG control demonstrated no immunolabeling, and an additional negative control with no primary antibody incubation similarly showed no immunolabeling. These results are in line with established spatial localizations of VSMCs.^{4,43} Interestingly, at week 2, the cells migrating into the lumen are not α -actin⁺, whereas, by week 3, all the cells within the neointima are α -actin⁺. No difference in α -actin expression can be seen between wildtype and Poldip2 (+/-) arteries in injured and uninjured arteries, which suggests that the pathological differences are unrelated to

basal and spatial localizations of VSMCs. Temporal differences in migration can not be surmised here as α -actin is not a migration marker; in fact, no clear marker of migration has been identified.

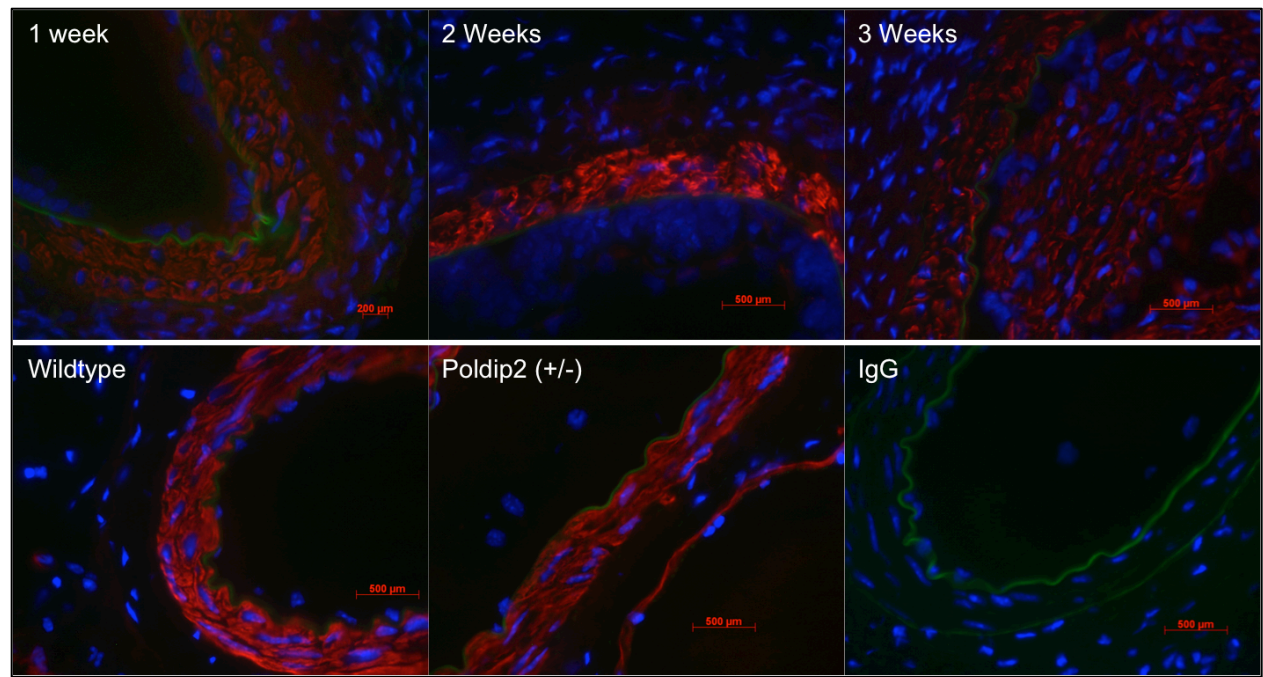


Figure 19- Smooth muscle cell α actin immunolabeling in Poldip2 (+/-) mice along the three-week time course (top line). Wildtype and Poldip2 (+/-) mice uninjured arteries express the same ubiquitous SMC α -actin within the medial layer. The IgG control demonstrates no immunoreactivity.

DISCUSSION

Neointima formation is an intricate process that involves multiple cellular dynamics. This wire injury model offers an alternative model of transluminal injury in mouse femoral arteries that was previously not possible with balloon transluminal injury due to the small size of mouse arteries.¹⁰ With a 95% success rate, rapid onset of medial cell apoptosis, and replicable neointimal hyperplasia with lesion formation ceasing ~3-4 weeks post-injury, this model is widely used and effective in understanding the mechanisms of restenosis.¹⁰ In this study, we looked at three cellular processes *in vivo* and *in vitro* that may be affected by Poldip2 expression during neointima development. These observations support the notion that Poldip2 expression is important in neointima formation. This study partially links Poldip2 expression to extracellular matrix accumulation in the neointima and potentially to proliferation, while it excludes its role in injury-mediated apoptosis, all of which may be involved in the pathology. As the roles of Poldip2 become clearer, the exact mechanism by which it propagates these cellular processes will help delineate which of Poldip2's regulatory interactions are of significance in cardiovascular pathology.

The production of extracellular matrix components is essential to the stability, structure, and contractility of the blood vessel. VSMCs are responsible for the synthesis and organization of the unique ECM present in mature large conducting vessels.⁴³ Once maturity and optimal vessel wall composition is reached, any VSMC stress-response remodeling leads to a change in ECM wall content due to an attempt to retain normal physiology. In neointima formation, this exact response is predicted to result in the adjustment of ECM components to counteract the wire injury.

Our results indicate that Poldip2 (+/-) animals demonstrate a higher amount of collagen fibers within the neointima at the three-week time point, the only time point that demonstrated neointimal birefringence. Collagens type I and III are responsible for providing structural support to the vessel, with collagen I mainly localized to the medial layer and collagen III mainly localized to the adventitia in normal vasculature. It has been shown that adventitial cells do not contribute to neointima formation;⁴⁴ it is therefore possible to link these collagen observations to the *in vitro* studies conducted by Dr. Datla, which showed an increase in collagen I secretion in VSMCs. Additionally, structural analysis of Poldip2 (+/-) aortic walls has shown that Poldip2 (+/-) aortas exhibit less uniform and fragmented elastin lamellae and express significantly more fibrillar/amorphous ECM components within the interlamellar area, as observed under transmission electron micrographs (unpublished data courtesy of Dr. Lu Hilenski). These observations suggest that Poldip2 exhibits a certain control of ECM integrity. Whether or not the differences observed in neointimal collagen deposition were due to the natural baseline differences in ECM organization between WT and Poldip2 (+/-) animals cannot be deduced from this study, especially when it is not known whether or not these differences confer a significant difference in arterial mechanical function.

It should be noted that the amount of collagen observed via birefringence in the neointima three weeks post surgery was minimal. Collagen birefringence of the developing neointima at the one-week and two-week time points was practically unobservable (data not shown). Even though the exact mechanism of neointima formation in a spatial and temporal context is not fully understood, it is pathologically feasible that collagen accumulation at the week one and week two time points is not yet relevant, given that neointima formation is not prominent until between day 14 and day 21 and is maximized 21 to 28 days post wire-injury.¹⁰

Nevertheless, well-formed, organized ECM is integral to SMC migration into the neointima, as the fibers form scaffolding for cellular processes integral to this process. It is possible that given the temporal relevance of this pathology, extremely thin collagen fibers recently deposited are not birefringent enough in the red hue to be estimated in the calculations. Nevertheless, by day 21, it appears as though collagen deposition in the neointima is increased in Poldip2 (+/-). Its physiological significance remains to be determined.

There are a few possible reasons for the minimal birefringence observed in the neointima at the three-week time point. Firstly, it is very likely that since the progression of neointimal hyperplasia occurs mainly between the two-week and three-week post injury time points, as observed by the minimal pathological progression of the condition at one week and two weeks post injury, the thinnest most recently produced collagen fibers may have been excluded from calculations. Secondly, baseline characteristics of femoral artery collagen conducted by Dr. Candace Adamo demonstrated very little quantifiable collagen within the medial layer of WT and Poldip2 (+/-) aortas using picrosirius red staining. In fact, most arterial collagen fiber quantifications described in the literature use larger arteries from larger animals, such as the iliac artery from rabbits.⁴⁰ Thirdly, even though collagens I-III are the targets of picrosirius red staining, collagen IV and fibronectin are of major importance in the vasculature, and may be more prevalent within the neointima than collagens I-III.⁴³ Future studies should be conducted to elucidate their relation to Poldip2 heterozygosity.

Because many cell types potentially contribute to neointima formation, the positive identification of smooth muscle α -actin as a marker of VSMCs within our AOIs is of extreme importance. The α -actin negative cells localized on the luminal side of the two week artery shown in Figure 19 (2 weeks) could be a combination of endothelial cells, T-lymphocytes,

monocytes, and/or fibroblasts, which are responsible for the initiation of SMC proliferation and migration. These mediators of neointima formation are initially recruited by the activation of SMCs, which then secrete growth mediators, matrix modulators, vasoactive substances, and inflammatory mediators that in turn recruit a number of leukocytes and more SMCs to proliferate and migrate in an attempt to remodel the damaged vessel. In this animal model of neointimal hyperplasia, these events are expected to occur around two weeks post injury. These α -actin negative cells should be considered when looking at the neointimal cell counts at the week one and week two post injury time points. They may explain over-estimations of neointimal cell counts, and why little collagen birefringence was seen at these time points. These findings were not applicable to the three-week neointima, as all cells of the neointima expressed α -actin, and subsequently expressed a significant difference in neointima development.

Our data on apoptosis of VSMCs suggests that Poldip2 functionality has no effect on apoptotic rates post wire-injury. Nox generated ROS in cell death mediation has been reported and may be linked to distinct pathological pathways, especially in cardiac myocytes of the failing heart where Nox4 is localized to the mitochondria,⁴⁵ but our data suggest that Poldip2 elicits no regulatory control over the initial cell death, which drives the beginning of the innate immune response to injury and leads to neointimal hyperplasia via VSMC activation. These results suggest that the initiating signals following injury are the same between each animal group, and that the pathological differences observed between each animal group must be due to the aforementioned ECM integrity, migration, and possible differences in VSMC proliferation.

With regard to VSMC proliferation, we characterized the percent of proliferating cells within the medial layer and neointima to get an idea of where proliferation is prominent and whether or not there is a spatial and temporal variation in proliferation based on Poldip2

functionality. The data collected are statistically inconclusive and will have to be supplemented with additional animals, but they suggest that proliferation by week three is completely attenuated. Proliferation peaked in the media at the two-week time point, and a trend of decreased proliferation is observed with heterozygosity (two-fold decrease, $P>0.05$). In fact, this trend holds within the medial layer of one-week animals (11.9% WT, 5.2% Poldip2 (+/-)), but the sample size is too small to confirm statistical relevance. The trend, however, is supported by *in vitro* studies, which show that Poldip2 downregulation attenuates proliferation in SMCs (unpublished data courtesy of Dr. Datla). When proliferation is pronounced in the neointima, there is no difference in the percentages of proliferating cells across the one-week and two-week time points and across genotypes. This can be explained by a simultaneous decrease in the amount of proliferating cells in the numerator and a decrease amount of total cells in the denominator. So, even though the percent proliferation is the same, there could potentially be fewer proliferating cells present within the neointima of Poldip2 (+/-) mice.

As noted, VSMC migration is also critical to neointima formation. Studying migration *in vivo* poses many problems, the main issue being that no migration marker has been identified. In fact, any conclusions on migration can only be made via comparisons to *in vitro* data and cellular pathways related to migration, such as focal adhesion turnover and extracellular matrix deposition. Either way, a concrete conclusion on whether or not VSMCs initially migrate from the medial layer and then proliferate into the lumen or first proliferate and then migrate, or even a combination of both, is difficult to make. Interestingly, the decrease in WT medial layer cells at one week compared to Poldip2 (+/-), may suggest that there may be a less pronounced onset of migration in the heterozygotes. The statistical significance of this trend needs to be applied to a larger sample size to determine any scientific relevance, but this observation would match the

role of Poldip2 in mediating migration by regulating focal adhesion turnover and ECM formation.

Along these lines, it is generally assumed that excess ECM accumulation contributes to the increase in neointima observed after injury. In this case, however, even though collagen production was increased, the thickness of the neointima was decreased. This suggests that the excess collagen impaired the ability of VSMCs to migrate into the neointima and proliferate, perhaps because the excess matrix is disorganized. Such an interpretation is supported by the ultrastructural studies alluded to above and the apparent reduction in medial proliferation (Figure 18) as measured by PCNA. The fact that Poldip2 (+/-) mice also have fewer cells in the neointima at day 21 (Figure 18) further suggests that medial cells may not be able to migrate into the neointima, a hypothesis consistent with *in vitro* work showing impaired migration in Poldip2-depleted cells.²⁹

By applying this injury model to Poldip2 (+/-) gene trap mice and observing the ensuing morphological differences in neointima formation, the pathological relevance of Poldip2 expression in VSMCs is clear. VSMCs express an intrinsic plasticity, which enables them to proliferate, migrate, produce extracellular matrix components, and respond to a multitude of environmental factors, all of which are integral to this pathological state and normal physiology. In fact, during development of the blood vessel, SMC plasticity plays a key role in morphogenesis.³³ VSMCs under normal physiological conditions are under the regulation of a wide array of hormonal and chemical signaling to maintain their differentiated phenotype, which is required for normal vascular function and morphology. In restenosis, this regulation is altered to the point of vascular dysfunction, and the role of Poldip2 in mediating neointimal hyperplasia is possibly centered on its regulation cytoskeletal organization and VSMC proliferation.

There are multiple molecular mechanisms by which Poldip2 heterozygosity could attenuate neointimal hyperplasia. First, Poldip2 was originally found to interact with the p50 subunit of DNA polymerase δ and with PCNA,³⁵ providing one mechanism by which Poldip2 heterozygosity might deregulate normal DNA replication. Poldip2 has also been shown to regulate spindle organization and chromosome segregation, an additional mechanism to control proliferation.^{35,36} Because Poldip2 also regulates Nox4, and Nox4 has been shown to promote cell survival by activating p38 mitogen-activated protein kinase (MAPK), serine/threonine kinase Akt/protein kinase B (Akt), and redox sensitive transcription factors, Nox4-linked pathways represent another potential mechanism for the control of proliferation by Poldip2.⁴⁶ Second, Poldip2 has clearly been linked to cytoskeletal remodeling and adhesion molecule expression, both of which are important in migration. Lyle et al²⁹ showed that Poldip2 regulates focal adhesion stability and stress fiber formation via a RhoA-dependent pathway, an indication that cytoskeletal effects are also mediated by this complex. In addition, surface expression of adhesion molecules for matrix interaction may be regulated by cytoplasmic shuttling, another potential function of Poldip2.³⁶ As both of these functions are mediated by Nox4, a redox component of the Poldip2 regulatory mechanisms seems likely. Which of these mechanisms contributes to the reduction of neointima formation in Poldip2 heterozygote mice remains to be determined, and will be the target of future studies. One thing is clear, however: Poldip2 function most likely plays a multifunctional role in the injury response.

Future directions and conclusions

These observations suggest that Poldip2 has many downstream effects that can be targeted for future studies. In addition to investigating the molecular pathways described above, it will be important to study regulation of gene expression of ECM proteins in Poldip2 heterozygote VSMCs. The generation of collagen fibers requires the activation and regulation of collagen α -chains, hydroxylating enzymes, metalloproteinases, lysyl oxidases, and chaperones that could be affected by this ablated genotype.⁴³ It is very possible and plausible that some of these genes are deregulated in this genetic model, and gene expression studies may provide a more concrete conclusion on this matter. These studies could provide a mechanistic link between Poldip2 heterozygotes and the observed increase in collagen deposition *in vitro*, and the *in vivo* abnormalities discussed in injured and uninjured vessel walls.

To augment and confirm studies on proliferation, future experiments should be designed to inject animals with bromodeoxyuridine (BrdU) prior to euthanasia. Although a successful protocol was developed, time-extensive troubleshooting for PCNA immunolabeling was necessary, and will most likely be necessary on an assay-dependent basis for future experiments. BrdU immunohistochemistry is selective for cells in the S phase only, and even though BrdU incorporation is necessary prior to tissue collection, the benefits are in the selectivity of the immunolabeling. Some of the issues associated with immunohistochemistry with PCNA or Ki67, another proliferation marker, is the presence of these antigens in the G₁ and G₂ phases of the cell cycle.⁴⁷ Although PCNA has been shown to be a good alternative to BrdU incorporation,^{48,49} it may overestimate the amount of proliferating cells and issues with immunoreactivity specificity could easily be avoided with BrdU or even [³H]thymidine labeling. Additionally, its potential

functional interaction with Poldip2 may influence labeling, so confirmation of PCNA results with a second method is desirable.

Furthermore, a Nox4 knockout genetic model has been developed since the start of this project. Future experiments following the same protocol of *in vitro* and *in vivo* analysis should be used to confirm these data, to see if Poldip2 heterozygosity corresponds to similar phenotypic disturbances in a Nox4 knock out model. Alternatively, Poldip2 (+/-) animals could be crossed with Nox4 transgenic animals in an attempt to reverse the phenotype. These experiments will delineate how much of the Poldip2 phenotype is due to dysregulation of Nox4 in normal physiology and aggravated pathology.

In conclusion, this study identifies two cellular functions that are targeted by Poldip2 heterozygosity, ECM production and stability, and proliferation, and omits another, apoptosis. Lyle et al²⁹ identified Poldip2 as a regulator of Nox4, and linked its functionality to cytoskeletal integrity and migration. Combined with this animal study, which is albeit limited by the number of animals used in each experiment, Poldip2 can be predicted to be involved in regulation of ECM integrity and reorganization in the pathological state, and be involved in the activation of VSMCs to proliferate within the medial layer. As more research is conducted on Nox4 and Poldip2 separately, the complete regulatory role of Poldip2 and the complete role of Nox4-generated ROS will become clearer, and illuminate some of the unspecified temporal and spatial properties of cellular functions in the pathological manifestation of restenosis.

REFERENCES

1. Kochanek KD, Xu J, Murphy SL, Minio AM, Kung HC. National vital statistics reports. *National Vital Statistics Reports*. 2011;59(4):1.
2. Roger VL, Go AS, Lloyd-Jones DM, et al. Heart Disease and Stroke Statistics, 2011 Update. About 1. About These Statistics2. American Heart Association's 2010 Impact Goals3. Cardiovascular Diseases4. Subclinical Atherosclerosis5. Coronary Heart Disease, Acute Coronary Syndrome, and Angina Pectoris6. Stroke (Cerebrovascular Disease) 7. High Blood Pressure8. Congenital Cardiovascular Defects9. Cardiomyopathy and Heart Failure10. Other Cardiovascular Diseases11. Family History and Genetics12. Risk Factor: Smoking/Tobacco Use13. Risk Factor: High Blood Cholesterol and Other Lipids14. Risk Factor: Physical Inactivity15. Risk Factor: Overweight and Obesity16. Risk Factor: Diabetes Mellitus17. End-Stage Renal Disease and Chronic Kidney Disease18. Metabolic Syndrome19. Nutrition20. Quality of Care21. Medical Procedures22. Economic Cost of Cardiovascular Disease23. At-a-Glance Summary Tables24. Glossary. *Circulation*. 2011;123(4):e18-e209.
3. Statistics NCfH. Health, United States, 2010: With Special Feature on Death and Dying. In: U.S. Department of Health and Human Services CfDCaP, ed. *Library of Congress*. Vol 76-641496. Hyattsville, MD2011.
4. Ross R, Glomset JA. The pathogenesis of atherosclerosis. *New England Journal of Medicine*. 1976;295(7):369-377.
5. Libby P. The Pathogenesis, Prevention, and Treatment of Atherosclerosis. In: Longo DL, Fauci, A.S., Kasper, D.L., Hauser, S.L., Jameson, J.L., Loscalzo, J., ed. *Harrison's Principles of Internal Medicine*. 18 ed. New York: McGraw-Hill; 2012.
6. Schillinger M, Minar E. Restenosis after percutaneous angioplasty: the role of vascular inflammation. *Vascular health and risk management*. 2005;1(1):73.
7. Popowich DA, Varu V, Kibbe MR. Nitric oxide: what a vascular surgeon needs to know. *Vascular*. 2007;15(6):324-335.
8. Weintraub WS. The pathophysiology and burden of restenosis. *The American journal of cardiology*. 2007;100(5):S3-S9.
9. Harrison D, Griendling, KK., Alexander, R. Biology of the Vessel Wall. In: Fuster V WR, Harrington RA, ed. *Hurst's The Heart*. 13th ed. New York: McGraw-Hill; 2011.
10. Sata M, Maejima Y, Adachi F, et al. A mouse model of vascular injury that induces rapid onset of medial cell apoptosis followed by reproducible neointimal hyperplasia. *Journal of molecular and cellular cardiology*. 2000;32(11):2097-2104.
11. Szocs K, Lassegue B, Sorescu D, et al. Upregulation of Nox-based NAD (P) H oxidases in restenosis after carotid injury. *Arteriosclerosis, thrombosis, and vascular biology*. 2002;22(1):21.
12. Majesky MW, Reidy MA, Bowen-Pope DF, Hart CE, Wilcox JN, Schwartz SM. PDGF ligand and receptor gene expression during repair of arterial injury. *The Journal of cell biology*. 1990;111(5):2149.
13. Lindner V, Reidy M. Proliferation of smooth muscle cells after vascular injury is inhibited by an antibody against basic fibroblast growth factor. *Proceedings of the National Academy of Sciences*. 1991;88(9):3739.
14. Halliwell B, Gutteridge J. [1] Role of free radicals and catalytic metal ions in human disease: An overview. *Methods in enzymology*. 1990;186:1-85.

15. Valko M, Leibfritz D, Moncol J, Cronin MTD, Mazur M, Telser J. Free radicals and antioxidants in normal physiological functions and human disease. *The international journal of biochemistry & cell biology*. 2007;39(1):44-84.
16. Bondia-Pons I, Ryan L, Martinez JA. Oxidative stress and inflammation interactions in human obesity. *Journal of Physiology and Biochemistry*. 2012:1-11.
17. Griendling KK, Sorescu D, Ushio-Fukai M. NAD (P) H oxidase: role in cardiovascular biology and disease. *Circulation research*. 2000;86(5):494-501.
18. Nunes GL, Robinson K, Kalynych A, King SB, Sgoutas DS, Berk BC. Vitamins C and E inhibit O₂-production in the pig coronary artery. *Circulation*. 1997;96(10):3593-3601.
19. Lee MY, Griendling KK. Redox signaling, vascular function, and hypertension. *Antioxidants & redox signaling*. 2008;10(6):1045-1059.
20. Selemidis S, Sobey CG, Wingler K, Schmidt HHHW, Drummond GR. NADPH oxidases in the vasculature: molecular features, roles in disease and pharmacological inhibition. *Pharmacology & therapeutics*. 2008;120(3):254-291.
21. Lee MY, Martin AS, Mehta PK, et al. Mechanisms of vascular smooth muscle NADPH oxidase 1 (Nox1) contribution to injury-induced neointimal formation. *Arteriosclerosis, thrombosis, and vascular biology*. 2009;29(4):480-487.
22. Papaharalambus CA, Griendling KK. Basic mechanisms of oxidative stress and reactive oxygen species in cardiovascular injury. *Trends in cardiovascular medicine*. 2007;17(2):48-54.
23. Rossi F, Zatti M. Biochemical aspects of phagocytosis in poly-morphonuclear leucocytes. NADH and NADPH oxidation by the granules of resting and phagocytizing cells. *Cellular and Molecular Life Sciences*. 1964;20(1):21-23.
24. Griendling KK, Minieri CA, Ollerenshaw JD, Alexander RW. Angiotensin II stimulates NADH and NADPH oxidase activity in cultured vascular smooth muscle cells. *Circulation research*. 1994;74(6):1141-1148.
25. Brown DI, Griendling KK. Nox proteins in signal transduction. *Free Radical Biology and Medicine*. 2009;47(9):1239-1253.
26. Lassègue B, Griendling KK. NADPH oxidases: functions and pathologies in the vasculature. *Arteriosclerosis, thrombosis, and vascular biology*. 2010;30(4):653-661.
27. Shi Y, Niculescu R, Wang D, Patel S, Davenpeck KL, Zalewski A. Increased NAD (P) H oxidase and reactive oxygen species in coronary arteries after balloon injury. *Arteriosclerosis, thrombosis, and vascular biology*. 2001;21(5):739-745.
28. Lassègue B, Clempus RE. Vascular NAD (P) H oxidases: specific features, expression, and regulation. *American Journal of Physiology-Regulatory, Integrative and Comparative Physiology*. 2003;285(2):R277.
29. Lyle AN, Deshpande NN, Taniyama Y, et al. Poldip2, a novel regulator of Nox4 and cytoskeletal integrity in vascular smooth muscle cells. *Circulation research*. 2009:CIRCRESAHA. 109.193722 v193721.
30. Serrander L, Cartier L, Bedard K, et al. NOX4 activity is determined by mRNA levels and reveals a unique pattern of ROS generation. *The Biochemical journal*. 2007;406(Pt 1):105.
31. Martyn KD, Frederick LM, von Loehneysen K, Dinauer MC, Knaus UG. Functional analysis of Nox4 reveals unique characteristics compared to other NADPH oxidases. *Cellular signalling*. 2006;18(1):69-82.

32. Clempus RE, Sorescu D, Dikalova AE, et al. Nox4 is required for maintenance of the differentiated vascular smooth muscle cell phenotype. *Arteriosclerosis, thrombosis, and vascular biology*. 2007;27(1):42-48.
33. Owens GK. Regulation of differentiation of vascular smooth muscle cells. *Physiological reviews*. 1995;75(3):487-517.
34. Klaile E, Kukalev A, Obrink B, Muller MM. PDIP38 is a novel mitotic spindle-associated protein that affects spindle organization and chromosome segregation. *Cell cycle*. 2008;7(20):3180-3186.
35. Liu L, Rodriguez-Belmonte EM, Mazloun N, Xie B, Lee MYWT. Identification of a novel protein, PDIP38, that interacts with the p50 subunit of DNA polymerase β and proliferating cell nuclear antigen. *Journal of Biological Chemistry*. 2003;278(12):10041.
36. Klaile E, Muller MM, Kannicht C, et al. The cell adhesion receptor carcinoembryonic antigen-related cell adhesion molecule 1 regulates nucleocytoplasmic trafficking of DNA polymerase delta-interacting protein 38. *Journal of Biological Chemistry*. 2007;282(36):26629-26640.
37. Renshaw S. Immunochemical staining techniques. *Immunohistochemistry*. Bloxham, UK: Scion Publishing. 2007:45-96.
38. Baum HP, Reichrath J, Theobald A, Schock G. Fixation requirements for the immunohistochemical reactivity of PCNA antibody PC10 on cryostat sections. *The Histochemical Journal*. 1994;26(12):929-933.
39. Junqueira LCU, Bignolas G, Brentani R. Picrosirius staining plus polarization microscopy, a specific method for collagen detection in tissue sections. *The Histochemical Journal*. 1979;11(4):447-455.
40. Rich L, Whittaker P. Collagen and picrosirius red staining: a polarized light assessment of fibrillar hue and spatial distribution. *Braz J Morphol Sci*. 2005;22(2):97-104.
41. Pickering JG, Weir L, Jekanowski J, Kearney M, Isner JM. Proliferative activity in peripheral and coronary atherosclerotic plaque among patients undergoing percutaneous revascularization. *Journal of Clinical Investigation*. 1993;91(4):1469.
42. Dispersyn GD, Ausma J, Thone F, et al. Cardiomyocyte remodelling during myocardial hibernation and atrial fibrillation: prelude to apoptosis. *Cardiovascular research*. 1999;43(4):947.
43. Wagenseil JE, Mecham RP. Vascular extracellular matrix and arterial mechanics. *Physiological reviews*. 2009;89(3):957-989.
44. De Leon H, Ollerenshaw JD, Griendling KK, Wilcox JN. Adventitial cells do not contribute to neointimal mass after balloon angioplasty of the rat common carotid artery. *Circulation*. 2001;104(14):1591-1593.
45. Ago T, Kuroda J, Pain J, Fu C, Li H, Sadoshima J. Upregulation of Nox4 by hypertrophic stimuli promotes apoptosis and mitochondrial dysfunction in cardiac myocytes. *Circulation research*. 2010;106(7):1253-1264.
46. Griendling KK, Sorescu D, Lassegue B, Ushio-Fukai M. Modulation of protein kinase activity and gene expression by reactive oxygen species and their role in vascular physiology and pathophysiology. *Arteriosclerosis, thrombosis, and vascular biology*. 2000;20(10):2175-2183.

47. Bravo R, Macdonald-Bravo H. Existence of two populations of cyclin/proliferating cell nuclear antigen during the cell cycle: association with DNA replication sites. *The Journal of cell biology*. 1987;105(4):1549-1554.
48. Muskhelishvili L, Latendresse JR, Kodell RL, Henderson EB. Evaluation of cell proliferation in rat tissues with BrdU, PCNA, Ki-67 (MIB-5) immunohistochemistry and in situ hybridization for histone mRNA. *Journal of Histochemistry & Cytochemistry*. 2003;51(12):1681.
49. Zeymer U, Fishbein M, Forrester J, Cercek B. Proliferating cell nuclear antigen immunohistochemistry in rat aorta after balloon denudation. Comparison with thymidine and bromodeoxyuridine labeling. *The American journal of pathology*. 1992;141(3):685.